

Forecasting SARS-CoV-2 Epidemic Dynamic in Poland with the pDyn Agent-Based Model

Karol Niedzielewski (✉ kniedzie@icm.edu.pl)

Interdisciplinary Centre for Mathematical and Computational Modelling, University of Warsaw,
<https://orcid.org/0000-0001-7405-2207>

Rafał P. Bartczuk

Interdisciplinary Centre for Mathematical and Computational Modelling, University of Warsaw,
<https://orcid.org/0000-0002-0433-7327>

Natalia Bielczyk

Ontology of Value <https://orcid.org/0000-0003-1604-9143>

Dominik Bogucki

Interdisciplinary Centre for Mathematical and Computational Modelling, University of Warsaw,
<https://orcid.org/0009-0000-9473-2242>

Filip Dreger

Interdisciplinary Centre for Mathematical and Computational Modelling, University of Warsaw,
<https://orcid.org/0000-0003-1812-8216>

Grzegorz Dudziuk

Interdisciplinary Centre for Mathematical and Computational Modelling, University of Warsaw,

Łukasz Górski

Interdisciplinary Centre for Mathematical and Computational Modelling, University of Warsaw,
<https://orcid.org/0000-0003-0871-6575>

Magdalena Gruzziel-Słomka

Interdisciplinary Centre for Mathematical and Computational Modelling, University of Warsaw,
<https://orcid.org/0000-0001-6882-7408>

Jędrzej Haman

Interdisciplinary Centre for Mathematical and Computational Modelling, University of Warsaw,

Artur Kaczorek

Interdisciplinary Centre for Mathematical and Computational Modelling, University of Warsaw,
<https://orcid.org/0000-0002-4752-4480>

Jan Kisielewski

Faculty of Physics, University of Białystok <https://orcid.org/0000-0002-1082-4324>

Bartosz Krupa

Interdisciplinary Centre for Mathematical and Computational Modelling, University of Warsaw,
<https://orcid.org/0000-0002-2958-2046>

Antoni Moszyński

Interdisciplinary Centre for Mathematical and Computational Modelling, University of Warsaw,
<https://orcid.org/0000-0003-0128-7384>

Jędrzej M. Nowosielski

Interdisciplinary Centre for Mathematical and Computational Modelling, University of Warsaw,
<https://orcid.org/0000-0002-9627-3008>

Maciej Radwan

Interdisciplinary Centre for Mathematical and Computational Modelling, University of Warsaw,
<https://orcid.org/0000-0001-5789-316X>

Marcin Semeniuk

Interdisciplinary Centre for Mathematical and Computational Modelling, University of Warsaw,
<https://orcid.org/0000-0002-3136-7249>

Urszula Tymoszuik

Division of Psychiatry, University College London <https://orcid.org/0000-0002-0781-2752>

Jakub Zieliński

Interdisciplinary Centre for Mathematical and Computational Modelling, University of Warsaw,
<https://orcid.org/0000-0001-8935-8137>

Franciszek Rakowski

Interdisciplinary Centre for Mathematical and Computational Modelling, University of Warsaw,
<https://orcid.org/0000-0001-6133-8900>

Research Article

Keywords: epidemic dynamics, epidemiology, agent-based model, COVID-19

Posted Date: November 14th, 2023

DOI: <https://doi.org/10.21203/rs.3.rs-2966996/v2>

License:   This work is licensed under a Creative Commons Attribution 4.0 International License.

[Read Full License](#)

Forecasting SARS-CoV-2 epidemic dynamic in Poland with the pDyn agent-based model

Karol Niedziewski^{1*}, Rafał P. Bartczuk^{1,2}, Natalia Bielczyk³, Dominik Bogucki¹, Filip Dreger¹, Grzegorz Dudziuk¹, Łukasz Górski¹, Magdalena Gruziel-Słomka¹, Jędrzej Haman¹, Artur Kaczorek¹, Jan Kisielewski^{1,4}, Bartosz Krupa¹, Antoni Moszyński¹, Jędrzej M. Nowosielski¹, Maciej Radwan¹, Marcin Semeniuk¹, Urszula Tymoszuik⁵, Jakub Zieliński¹, Franciszek Rakowski¹

*For correspondence:

k.niedziewski@icm.edu.pl (K)

¹Interdisciplinary Centre for Mathematical and Computational Modelling, University of Warsaw, Warsaw, Poland; ²Institute of Psychology, John Paul II Catholic University of Lublin, Lublin, Poland; ³Ontology of Value, Nijmegen, Netherlands; ⁴Faculty of Physics, University of Białystok, Białystok, Poland; ⁵Division of Psychiatry, University College London, London, Great Britain

Abstract We employ pDyn, an agent-based epidemiological model, to forecast the fourth wave of the SARS-CoV-2 epidemic, primarily driven by the Delta variant, in Polish society. The model captures spatiotemporal dynamics of the epidemic spread, predicting disease-related states based on pathogen properties and behavioral factors. We assess pDyn's validity, encompassing pathogen variant succession, immunization level, and the proportion of vaccinated among confirmed cases. We evaluate its predictive capacity for pandemic dynamics, including wave peak timing, magnitude, and duration for confirmed cases, hospitalizations, ICU admissions, and deaths, nationally and regionally in Poland. Validation involves comparing pDyn's estimates with real-world data (excluding data used for calibration) to evaluate whether pDyn accurately reproduced the epidemic dynamics up to the simulation time. To assess the accuracy of pDyn's predictions, we compared simulation results with real-world data acquired after the simulation date. The findings affirm pDyn's accuracy in forecasting and enhancing our understanding of epidemic mechanisms.

Introduction

The first confirmed case of coronavirus disease 2019 (COVID-19) in Poland was identified on March 4, 2020, approximately a month behind Western Europe countries (*Ministerstwo Zdrowia, 2020*) (cf. 1(a)). On March 10, the World Health Organization declared the local transmission of severe acute respiratory syndrome coronavirus 2 (SARS-CoV-2) in Poland (*Pinkas et al., 2020*). Within two days, the country recorded its first COVID-19-related fatality (*Duszyński et al., 2021*). As the epidemic spread, Poland's government declared an epidemic emergency, subsequently introducing mitigation policies (*Pinkas et al., 2020*) (see *Figure 1(d)*). Critical pharmaceutical and non-pharmaceutical interventions (NPIs) implemented between March 4, 2020, and December 31, 2021, are detailed in *Table 1* in the *Appendix 1*. These measures primarily included isolating infected individuals, quarantining contacts (with basic contact tracing), and SARS-CoV-2 testing. Public social distancing

41 measures, such as gathering bans and school and workplace closures, began in the second week
 42 of March 2020, culminating in a national lockdown on March 24, 2020. Further mandates for in-
 43 door and outdoor face coverings followed on March 30 and April 14, 2020. The national COVID-19
 44 vaccination program commenced on December 27, 2020.

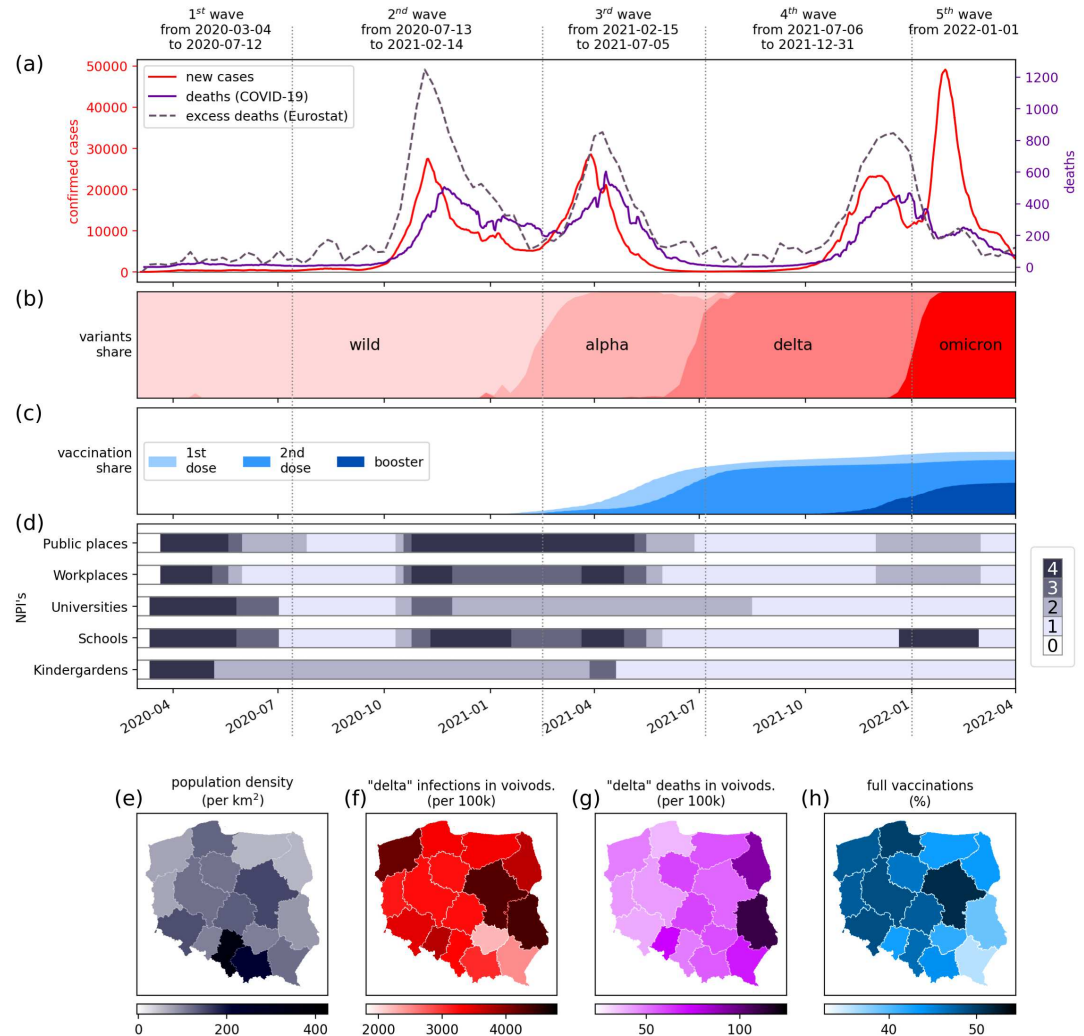


Figure 1. Timeline of SARS-CoV-2 epidemic in Poland. (a): The epidemic curve showing the progression of reported daily new confirmed cases in Poland (red), number of COVID-19-related deaths (purple), and excess mortality (dashed). (b): Proportions of dominating variants. (c): Full vaccination share. (d): Government mitigation measures by implementation areas and ranks of restrictive strength. (e): Map of inhabitants density in voivodships. (f): Map of reported cases during the Delta wave in voivodships. (g): Map of deaths during the Delta wave in voivodships. (h): Map of vaccinations per 100,000 inhabitants in voivodships up to May 2022.

Data sources: Daily cases & COVID-19-related deaths: Ministry of Health <https://gov.pl/web/koronawirus/wykaz-zarazen-koronawirusem-sars-cov-2>. Vaccinations: . Excess mortality: Eurostat (*Eurostat, 2023b*). SARS-CoV-2 variants: GISAID study (*Khare et al., 2021*). Mitigation measures: own elaboration based on governmental information please see *Table 2* in the *Appendix 1*.

45 The evolving nature of the epidemic, with factors such as new virus variants, seasonal transmis-
 46 sion fluctuations, regional outbreaks, and the introduction of vaccinations, necessitated a dynamic
 47 approach to epidemic mitigation. This approach involved localized and reactive strategies. For in-

48 stance, a reactive policy was initiated on August 7, 2020, with school closures and remote work man-
49 dates triggered by defined case thresholds per 10,000 inhabitants in administrative units. Compli-
50 ance with prevention measures, including face mask use, exhibited temporal and demographic
51 variations. Older adults, urban areas, and different epidemic stages demonstrated varying levels
52 of adherence (*Haischer et al., 2020; Delussu et al., 2022*).

53 Moreover, ongoing research on SARS-CoV-2 pathogen properties, such as transmission modes,
54 asymptomatic case infectivity, naturally induced immunity, its duration, and reinfection risks, added
55 to the complexity of forecasting SARS-CoV-2 spread. Consequently, the demand for accurate fore-
56 casts, encompassing new infections, hospitalizations (general and intensive care units [ICUs] ad-
57 missions), and COVID-19-related fatalities, intensified in response to the imperative of managing
58 SARS-CoV-2 transmission.

59 Agent-based models (ABMs) have been a robust method for modeling infectious disease spread
60 for over three decades (*Fox et al., 1971; Elveback et al., 1976*). They offer a direct representation
61 of dynamic social networks of agents and their heterogeneous interactions across georeferenced
62 locations (*Dilaver and Gilbert, 2023; Epstein, 1999; Millington et al., 2012*). These models often
63 rely on synthetic societies that mirror the demographic structure of specific territories (*Banks and*
64 *Hooten, 2021*). They usually incorporate dynamic microsimulation methodology with elements of
65 agent-based modeling. However, due to the convergence of these concepts, particularly as mi-
66 crosimulation becomes more and more intricate (*Railsback and Grimm, 2019; Richiardi, 2014; Vin-*
67 *cenot, 2018*), we employ the term "agent-based model" as an umbrella term in this article. ABMs
68 require input from a georeferenced network of setting where agents can operate and interact, like
69 households, schools, workplaces, and public spaces, referred to as contexts. ABMs, as generative
70 models, excel in replicating complex outbreak phenomena, accounting for regional disparities, de-
71 mographic structure, behavioral responses, and parameter calibration at finer spatial scales. In
72 contrast, data-based, phenomenological models, such as uniform mixing compartment models,
73 lack implicit interactions among crucial factors like virus variants and social networks (*Silverman*
74 *et al., 2021*).

75 The ABM developed by the Ferguson group (*Ferguson et al., 2005*) stands as a textbook ABM
76 approach for modeling infectious disease processes. Designed initially for simulating influenza
77 spread and assessing the effectiveness of targeted antiviral prophylaxis in Southeast Asia, this
78 model classifies individuals into households with distinct generational layers. In 2020, it underwent
79 adaptation to predict SARS-CoV-2 transmission dynamics by adjusting disease parameters to align
80 with the virus's characteristics *Ferguson et al. (2020)*. These forecasts informed the intermittent
81 lockdown strategy in the UK, known as "The Hammer and the Dance" (*Pueyo, 2020*).

82 Agent-based models (ABMs) have proven effective in modeling and predicting epidemics. They
83 function as virtual laboratories that enable the formalization and testing of epidemic dynamics (*Priese-*
84 *mann et al., 2021*). Unlike models that rely on general factors and aggregate variables, ABMs focus
85 on modeling individual agents and their interactions, allowing for the development of agent-level
86 theories, identification of fundamental principles and assumptions, and uncovering research gaps
87 and inconsistencies in theoretical systems (*Dilaver and Gilbert, 2023; Epstein, 1999; Frias-Martinez*
88 *et al., 2011*). Consequently, the prediction accuracy of ABMs depends on accurately representing
89 elementary epidemic processes and supporting hypotheses regarding their impact on real-world
90 data (*Dilaver and Gilbert, 2023; Epstein, 1999; Millington et al., 2012*). However, implementing
91 complex epidemic processes and adhering to real-world rules come at the cost of numerous pa-
92 rameters and high computational expenses. Additionally, the calibration process poses a signifi-
93 cant challenge, demanding substantial resources to achieve reliable calibration (*Millington et al.,*
94 *2012; Macal, 2016; Epstein, 1999*).

95 Our initial model, known as pDyn (derived from "pandemics dynamics"), was developed in 2008
96 to depict influenza spread scenarios in Poland (*Rakowski et al., 2010a,b*), drawing inspiration from
97 the Ferguson group model (*Ferguson et al., 2005*). In response to the COVID-19 pandemic, we
98 adapted this simulation platform to meet the specific requirements of decision-makers based on

99 the pandemic's unique characteristics (*Niedziewski et al., 2022*). The model can simulate and
100 forecast various SARS-CoV-2 transmission scenarios. The pDyn model has received official endorse-
101 ment from the government, alongside the MOCOS model (*Adamik et al., 2020*) and the Ministry of
102 Health Department of Analysis and Strategy model, as one of the primary tools for providing scien-
103 tific insights and epidemic forecasts to policymakers and medical advisory councils on a long-term
104 basis.

105 In Poland, several ABM models have been developed. Compared to the MOCOS model (*Adamik*
106 *et al., 2020*), pDyn distinguishes itself with a detailed and georeferenced structure of various con-
107 texts, while MOCOS incorporates advanced contact-tracing analytical methods. Other models,
108 such as those developed as conceptual models (*Pałka et al., 2022; Regulski et al., 2021*) offered
109 valuable methodological insights but were primarily employed locally and did not transition into
110 operational use.

111 During the initial year of the pandemic, the pDyn model stood out as one of the few robust
112 models subjected to validation against real-world data. A systematic review of 126 SARS-CoV-2
113 ABMs highlighted that only 17% underwent validation against real-world data, 3% were compared
114 with other models, and 2% underwent systematic testing (*Lorig et al., 2021*). Furthermore, pDyn
115 has continuously undergone external validation with real-world data as part of the German and
116 Polish COVID-19 Forecast Hub since November 2020 (*Bracher et al., 2021, 2022*). Both ABMs, pDyn
117 and MOCOS, have demonstrated significant performance improvements in long-term case fore-
118 casting in Poland, thanks to their tailored approaches adapted to the specific circumstances of the
119 country (*Bracher et al., 2022*).

120 As for other single-country ABM models across European states, numerous models are dedi-
121 cated to Austria (*Bicher et al., 2018, 2023*), Germany (*Müller et al., 2021; MONID - MOdeling Net-*
122 *work for severe Infectious Diseases, 2023*), Spain (*Singh et al., 2022; Merino et al., 2023*), France (*Ho-*
123 *ertel et al., 2020*), UK (*Ferguson et al., 2020*), Italy (*Bouchnita and Jebrane, 2020; Giacobelli, 2021;*
124 *Lombardo et al., 2022; Fazio et al., 2022*) and Ireland (*Novakovic and Marshall, 2022*). However,
125 these models are tailored to countries other than Poland (or their respective regions) and have not
126 undergone validation within the European COVID-19 Forecast Hub (*Sherratt et al., 2023*). There-
127 fore, comparing the performance and validity of these models with pDyn in a meaningful manner
128 would be challenging, if not impossible. Nonetheless, considering the population size of European
129 nations, pDyn ranks among the top 10 in terms of simulated populations.

130 This report utilizes the ABM pDyn to forecast the spatiotemporal dynamics of the COVID-19 epi-
131 demic in Poland. Our methodology encompasses disease transmission, disease progression, and
132 epidemic course (see *Figure 2*). Disease transmission considers multi-variant pathogens, partial
133 immunity, and social contacts. The disease progression component includes a detailed represen-
134 tation of disease-related states, age-dependency, and dark figure estimation. Lastly, the epidemic
135 course encompass changes in risk exposure due to NPIs or other shifts in behavior, vaccination
136 policies, cross-immunity, and immunity waning. We validate the dynamics implemented in the
137 model by inspecting their consistency with real-world data not used for calibration. Many of these
138 features are model enhancements related to COVID-19 epidemics (indicated by asterisks * in *Fig-*
139 *ure 2*).

140 This investigation spans from the onset of the epidemic to the end of 2021, covering four SARS-
141 CoV-2 waves in Poland. The first and second waves (March 4, 2020–July 12, 2020, and July 13,
142 2020–February 14, 2021) were driven by the wild-type virus variant, followed by the third wave
143 with the Alpha variant (February 15, 2021–July 5, 2021) and the fourth wave with the Delta vari-
144 ant (July 6, 2021–December 31, 2021). During this period, Poland reported 4,106,914 SARS-CoV-2
145 cases, 96,967 COVID-19-related deaths, and 173,376 total excess deaths (*Ritchie et al., 2020*) (see
146 *Figure 1(a)* and (b)).

147 The forecast, formulated on October 28, 2021, using pDyn (*Niedziewski et al., 2022*), targets
148 the fourth (Delta) wave of the epidemic in Poland. This wave is noteworthy as it subsided sponta-
149 neously, without the imposition of restrictions or contact limitations, signifying the attainment of



Figure 2. Features of the current version of the pDyn model. The model encompasses three main classes of features: (1) *Disease transmission*, which incorporates airborne transmission dynamics, multi-variant pathogens, vaccine characteristics, partial immunity, and social contacts structure; (2) *Disease progression*, which models disease-related states, their durations and transition probabilities, age-dependency, and estimates of underreporting; and (3) *Epidemic course*, modeling changes in risk exposure, vaccination policies, cross-immunity, and immunity waning. Many of these components represent enhancements related to COVID-19 epidemics (indicated by asterisks [*]) compared to the original model version.

150 herd immunity. Subsequent waves in 2022 represented reinfections and conveyed reduced risks
 151 of severe illness and death due to decreased susceptibility to new variants. The forecast did not
 152 include the emerging Omicron wave in January 2022 due to a lack of information on this variant
 153 at that time. To be precise, Omicron variant was not introduced to the forecast of interest, formu-
 154 lated on October 28, 2021. Therefore, any comparison between the forecast and real-world data
 155 should only consider the period until December 31, 2021, as the Omicron variant emerged in early
 156 2022.

157 This study aimed to achieve three specific objectives: (1) assessing the validity of the dynamics
 158 embedded in the pDyn model, (2) evaluating its capacity to predict the dynamics of disease-related
 159 states at the national level, and (3) gauging its ability to predict epidemic dynamics in Poland's high-
 160 est administrative units (voivodships) using nationally reported data. We compared real-world data
 161 on SARS-CoV-2 variants, immunization dynamics, and the ratio of vaccinated individuals among
 162 confirmed cases with our model's estimates to assess its validity. Additionally, we compared simu-
 163 lation results with real-world data obtained after the simulation date to evaluate pDyn's predic-

164 tive accuracy. We also assessed regional forecasts made using nationally reported data, taking
 165 into account the synthetic society's reflection of geographical variations in the social-demographic
 166 structure of the Polish population.

167 As demonstrated, the generative, epidemiology-driven dynamic approach of pDyn achieved
 168 high predictive accuracy when modeling the spread of COVID-19 epidemics.

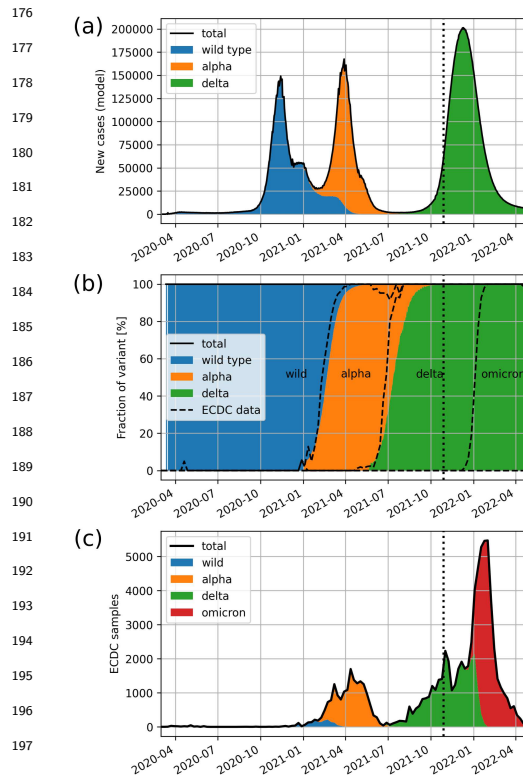
169 Results

170 Evaluation of the model validity

171 In this section, we assess the validity of the model's dynamics by comparing its outputs with real-
 172 world data pertaining to the dominant variant of concern, immunization levels, and the fraction of
 173 vaccinated detected cases.

174 Dominating variant of pathogen

175



176
177
178
179
180
181
182
183
184
185
186
187
188
189
190
191
192
193
194
195
196
197
198
199
200
201
202
203
204
205
206
207
208
Figure 3. Comparison of the dynamics of a succession of SARS-CoV-2 variants obtained from the pDyn model (colors) with the dataset obtained from GISAID study (dashed lines). All the data is aggregated in weekly intervals. The vertical dotted line marks the simulation date.

Data source: GISAID study (Khare et al., 2021)

209 Immunization level

210 The immunization dynamics during the epidemic originating from the pDyn model, categorized
 211 as disease-induced, vaccination-induced, and total immunization, are presented in **Figure 4**. This

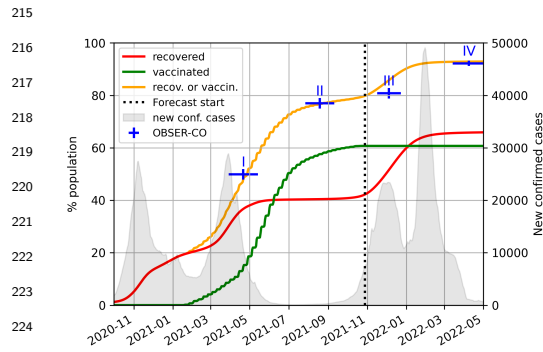
Before the simulation date, three predominant variants had been identified in Poland: the wild type, Alpha, and Delta. In **Figure 3(a)**, the distribution of these variants (wild type [blue], Alpha [orange], and Delta [green]) among infected agents is depicted. Panel (b) compares the model's variant succession dynamics with real-world data from GISAID (Khare et al., 2021). This assessment excludes the Omicron variant, which was not part of our October 2021 forecast.

Given that GISAID data relies on samples of varying sizes and considering potential biases in the data due to relatively small samples for Poland (as shown in **Figure 3(c)**), we primarily compared the relative prevalence of variants, expressed as percentages. To validate our findings, we compared the timing of variant succession at the 25%, 50%, and 75% percentile thresholds.

The pDyn model reached 25% prevalence of the Alpha variant one week after the reference GISAID data, while it reached 50% and 75% prevalence two weeks after the reference GISAID data.

Regarding the Delta variant, our model reached 25% prevalence two weeks after the reference GISAID data, 50% prevalence three weeks after, and 75% prevalence four weeks after the reference GISAID data. This transition from the Alpha to Delta variant occurred during a period of relatively low newly detected cases, supporting the realism of our model's predictions.

212 model output is systematically compared with data from the OBSER-CO nationwide seroprevalence
 213 study conducted by the National Institute for Public Health in Poland (*National Institute of Public*
 214 *Health, 2021*).



226 **Figure 4.** Comparison of immunization dynamics
 227 between the model output and the OBSER-CO study.
 228 The lines show the cumulative percentage of the
 229 agents (left axis) that are recovered (red),
 230 vaccinated (green), or recovered or vaccinated
 231 (yellow). The blue markers indicate the estimated
 232 fraction of the population with SARS-CoV-2-
 233 specific antibodies from four rounds of the
 234 OBSER-CO study. The horizontal marker line
 235 denotes the duration of each round, the
 236 vertical one represents the 95% confidence
 237 interval of the estimate. A vertical dotted line
 238 indicates the simulation date. The gray shape
 239 represents the number of real-world confirmed
 240 cases (right axis).

241 Data source: OBSER-CO study (*National Institute of Public Health, 2021*)

242 Fraction of vaccinated detected cases

243 The third validation involves assessing the frac-
 244 tion of vaccinated detected cases, which refers
 245 to the number of vaccinated individuals among
 246 all infected and detected individuals. The
 247 model adopted a vaccination strategy based
 248 on government data, which included the num-
 249 ber of vaccinated agents at specific ages,
 250 times, and locations. However, the dynamics
 251 of the fraction of vaccinated detected cases
 252 emerged from the model and could be com-
 253 pared to real-world data (obtained under a
 254 non-disclosure agreement). The comparison
 255 between the model's outcomes and epidemio-
 256 logical data regarding the fraction of vac-
 257 cinated detected cases is presented in *Figure 5*.

258 Generally, the dynamics obtained from the
 259 pDyn model align closely with the epidemio-
 260 logical data. The mean absolute error from
 261 January 1, 2021, to October 28, 2021 (forecast

Figure 4 reveals a close alignment between
 the cumulative sum of recovered and vac-
 cinated individuals predicted by the model and
 the estimates derived from the seroprevalence
 study at all four study rounds. The percent-
 age of the entire population represented by
 these estimates is as follows: 48.1 (model) vs.
 49.9 (study, 95% CI [47.9; 51.9]) in April/May
 2021, 76.8 (model) vs. 77.0 (study, 95% CI
 [75.0; 79.0]) in September 2021, 85.8 (model)
 vs. 80.8 (study, 95% CI [78.8; 82.8]) in Decem-
 ber 2021, and 92.9 (model) vs. 92.2 (study,
 95% CI [91.2; 93.2]). Notably, rounds I and II
 of the OBSER-CO study fell within the cali-
 bration stage of the simulation. In contrast,
 the model results for rounds III and IV are
 purely prognostic values.

It is important to acknowledge that the
 OBSER-CO study primarily focuses on sero-
 prevalence, which relies on antibody levels in
 trial groups, differing somewhat from the in-
 dicator of the sum of recovered and vac-
 cinated cases obtained from the model. Never-
 theless, the significant alignment between the
 model's approximation of societal immunity
 and OBSER-CO data underscores the model's
 reliability in forecasting future epidemic waves
 despite these variations in indicators.

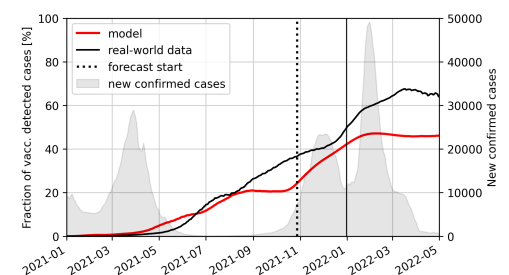


Figure 5. Comparison between the fraction of
 vaccinated detected cases generated from the pDyn
 (red line) and epidemiological data (black line).
 The vertical dotted line indicates the simulation date,
 and the solid vertical line — the end of the
 estimation period for the model-to-real-data fit
 indices. The gray shape in the background
 represents the number of real-data new cases.

262 date) equals 3.44%; from October 29, 2021, to December 31, 2021, equals 7.23%; and from Jan-
 263 uary 1, 2022, equals 16.34%. The maximal error from January 1, 2021, to October 28, 2021, equals
 264 14.01%; from October 29, 2021, to December 31, 2021, equals 12.20%; and from January 1, 2022,
 265 equals 21.69%. The larger maximal error before the forecast date may have been due to data vari-
 266 ability when the number of cases was still low, but vaccination uptake had reached its saturation
 267 point (**Figure 4**, green line).

268 The quantitative indices used to validate the Delta wave forecast were estimated until Decem-
 269 ber 31, 2021, when the Omicron wave officially began. Considering the whole period (from Jan-
 270 uary 1, 2021, until May 1, 2022), the maximal error occurred on March 17, 2022, after the Delta
 271 domination period. Given that the Omicron variant was not considered in the forecast, the most
 272 considerable discrepancy between our simulation and real-world data was expected to occur after
 273 December 31, 2021.

274 Prediction of the epidemic dynamics during the Delta wave on the national level

275 In this section, we evaluate the accuracy of the pDyn forecast by comparing its results with real-
 276 world data for new confirmed cases, COVID-19-related deaths, hospitalized patients, and ICU pa-
 277 tients published by the Ministry of Health. Visualizations of the forecast for the Delta-wave (**Fig-
 278 ure 6**) and the entire epidemic (**Figure 6—figure Supplement 1**) are presented. To assess the
 279 model's performance, we conducted a comparative analysis with real-world data, emphasizing the
 280 accuracy of peak timing, magnitude, and duration, with summarized results in **Table 1**.

Table 1. The comparison between pDyn simulation results and epidemiological data (see text) for disease-related states regarding the peak value, peak date, and width in terms of the Full-Width Half-Maximum (FWHM) of the Delta wave in Poland. All data is reported daily. Real-world numbers of reported deaths and excess deaths are compared to the same number of COVID-19-related deaths from the simulation.

Output	Comparison	Peak value	Peak timing	Width (FWHM)
New confirmed cases	Simulation	25770	2021-12-05	68
	Real-world	24120	2021-11-29	45
	Difference	1659	6	23
	Relative difference	6.84%		51.11%
Hospitalized	Simulation	41315	2021-12-12	66
	Real-world	23520	2021-12-10	61
	Difference	17795	2	5
	Relative difference	75.66%		8.20%
ICU patients	Simulation	5311	2021-12-21	66
	Real-world	2115	2021-12-14	67
	Difference	3196	7	-1
	Relative difference	151.11%		-1.49%
Reported deaths	Simulation	889	2021-12-21	68
	Real-world	443	2021-12-17	62
	Difference	446	4	6
	Relative difference	100.68%		9.68%
Excess deaths	Simulation	889	2021-12-21	68
	Real-world	845	2021-12-10	66
	Difference	44	11	2
	Relative difference	5.21%		3.03%

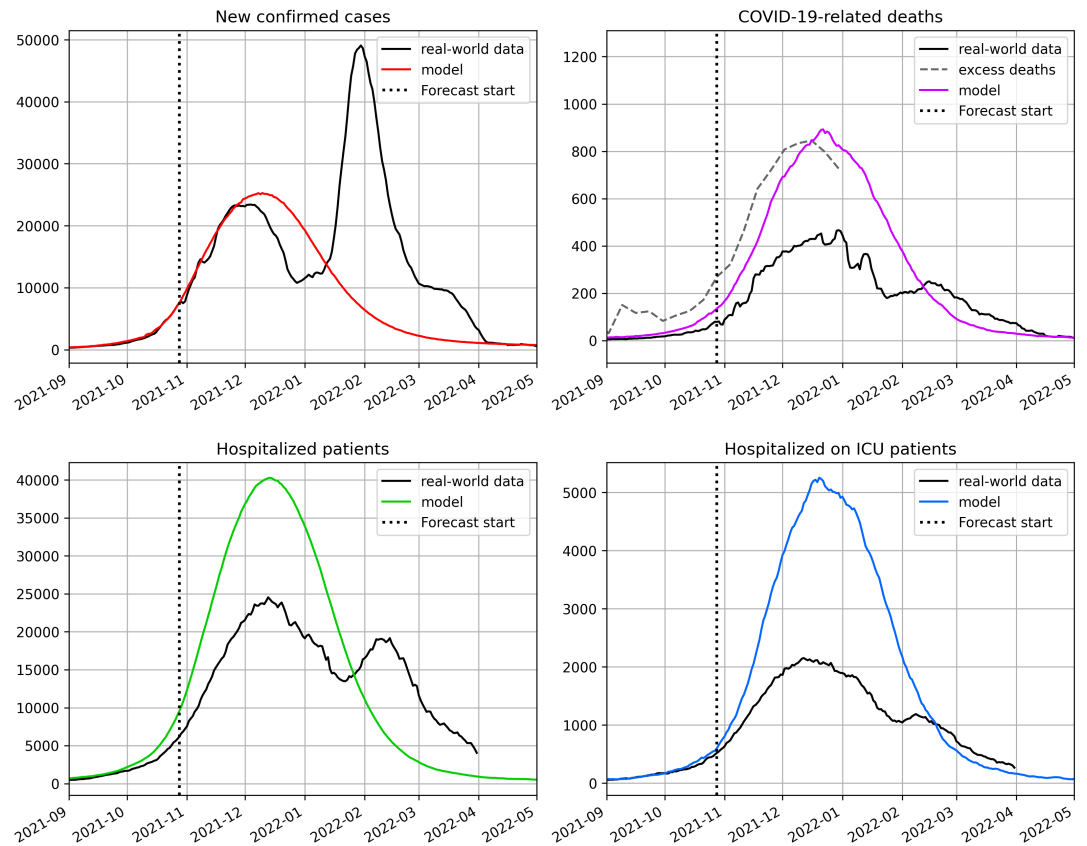


Figure 6. Comparison between the output generated from the model (colored lines) and the COVID-19 data from the Polish Ministry of Health (black) and Eurostat (dashed gray) for the Delta wave of the COVID-19 epidemics in Poland. Top left: new detected cases. Top right: deaths. Bottom left: hospitalized patients. Bottom right: ICU patients. The vertical dotted line marks the simulation date.

Data source: Eurostat (*Eurostat, 2023a*) **Figure 6—figure supplement 1.** Comparison between the pDyn model-generated output and the epidemiological data for the entire course of the COVID-19 epidemics in Poland.

281 The forecasted peak values tended to be overestimated, with the most accurate prediction for
 282 new cases (a relative difference of $\sim 7\%$) compared to other metrics. As shown in **Figure 6**, the
 283 predicted number of hospitalized patients, ICU patients, and COVID-19-related deaths exceeded
 284 the official data provided by the Ministry of Health: hospitalizations by approximately 76%, ICU ad-
 285 missions by around 151%, and COVID-19-related deaths by roughly 101%. Concerning the timing
 286 of peaks, our predictions were most accurate for hospitalized patients (with a 2-day difference),
 287 followed by reported deaths (4 days), new confirmed cases (6 days), and ICU patients (7 days).
 288 The forecasted wave length, as measured by the Full-Width Half-Maximum (FWHM), was the most
 289 accurate for ICU patients (approximately 1%) and hospitalized patients (around 8%), followed by
 290 reported deaths (approximately 10%) and new cases (about 51%). Notably, the relative difference
 291 in FWHM between the modeled and observed new confirmed cases was likely due to the holiday
 292 period in late December 2021, leading to a lower testing rate and detection ratio than before the
 293 holidays. Given that our model assumes a constant detection ratio, the real-life decrease in report-
 294 ing likely contributed to the observed discrepancy in the confirmed cases' wave length.

295 It is important to emphasize that the model's primary aim was not to predict the actual number
 296 of hospitalized and ICU patients but to estimate their expected numbers. Therefore, this distinc-
 297 tion should be kept in mind when interpreting the results, as it may explain the significant differ-

298 ences between the model's peak value predictions for hospital and ICU beds and the real-world
299 data. Nonetheless, the predictions regarding the peak timing of hospitalized and ICU patients
300 demonstrated that our forecast accurately captured the dynamics of the Delta wave. We relied
301 on occupied beds, rather than hospital admissions, to assess hospitalizations since the Ministry of
302 Health only provided data on occupied beds. A similar limitation affected our assessment of ICU
303 hospitalizations.

304 Moreover, we found that excess deaths were a more reliable parameter than officially reg-
305 istered COVID-19 deaths. Consequently, we present the forecast of COVID-19-related deaths in
306 comparison to estimates of excess deaths as defined by Eurostat *Eurostat (2023b)*: "Excess mor-
307 tality is the rate of additional deaths in a month compared to the average number of deaths in the
308 same month over a baseline period (2016-2019)." A positive value indicates an increase in deaths
309 compared to the baseline, while a negative value signifies fewer deaths compared to the baseline
310 period. For a more accurate quantitative comparison, we provided data in weekly resolution com-
311 puted using Eurostat weekly excess deaths data. The quantitative estimates of peak timing, peak
312 value, and wave length are presented in the lower panel of *Table 1*. Notably, the predicted number
313 of deaths more closely followed excess deaths than reported deaths in terms of the peak value (a
314 relative difference of approximately 5% vs. approximately 101%) and wave length (around 3% vs.
315 approximately 10%).

316 **Prediction of the epidemic dynamics during Delta wave on regional level**

317 Here, we demonstrate the model's capability to forecast epidemic dynamics of disease-related
318 states in voivodships while using national-level epidemic data for calibration. The regional trajec-
319 tories of pDyn outputs diverged due to synthetic society's spatial structure, vaccination process,
320 regional variation in weight multipliers (accounting for differences in NPIs implemented before
321 the Delta wave), and the locations of initial infections for each introduced variant in the simulation.

322 For a comprehensive comparison between the data generated by the model and real-world
323 data throughout the entire course of the epidemic in voivodships (comprising the total number of
324 detected cases, COVID-19-related hospitalizations, COVID-19-related ICU occupation, and COVID-
325 19-related deaths), please refer to *Appendix 2*. Detailed quantitative comparisons of peak timing,
326 peak value, and wave length are also included in Tables in *Appendix 2*. In this context, *Figure 7*
327 primarily presents the summary statistics of model accuracy at the regional level.

328 The top panel of *Figure 7* illustrates the distributions of peak values, peak dates, and FWHM val-
329 ues in voivodships, obtained from both the model (upward distributions) and real-life data (down-
330 ward distributions). For clarity, the bottom panel shows these data as distributions of absolute
331 differences (for peak date) or relative differences (for peak value and FWHM) between the model
332 and real-life data.

333 The medians of the difference distributions, indicated by vertical black lines in the bottom panel
334 of *Figure 7*, broadly align with the differences reported at the national level. Notably, there are a
335 few outliers in the graphs depicting relative differences in peak value and FWHM for newly detected
336 cases, hospitalized patients, and deaths.

337 Upon inspecting the difference distributions (bottom panel in *Figure 7*), particularly the relative
338 peak value difference (left plot) concerning detected cases, occupied beds, and deaths, one can ob-
339 serve a clear outlier in each plot, which corresponds to Podkarpackie voivodeship. The substantial
340 relative differences observed across voivodeships may be partially attributed to regional behav-
341 ioral factors, such as varying levels of willingness to undergo COVID-19 testing or seek hospital
342 treatment for COVID-19, compared to other regions in the country.

343 On average, the pDyn model demonstrates convergence with real-world data and predicts the
344 number of newly detected cases at the individual voivodeship level with lower accuracy than the
345 predictions made at the national level.

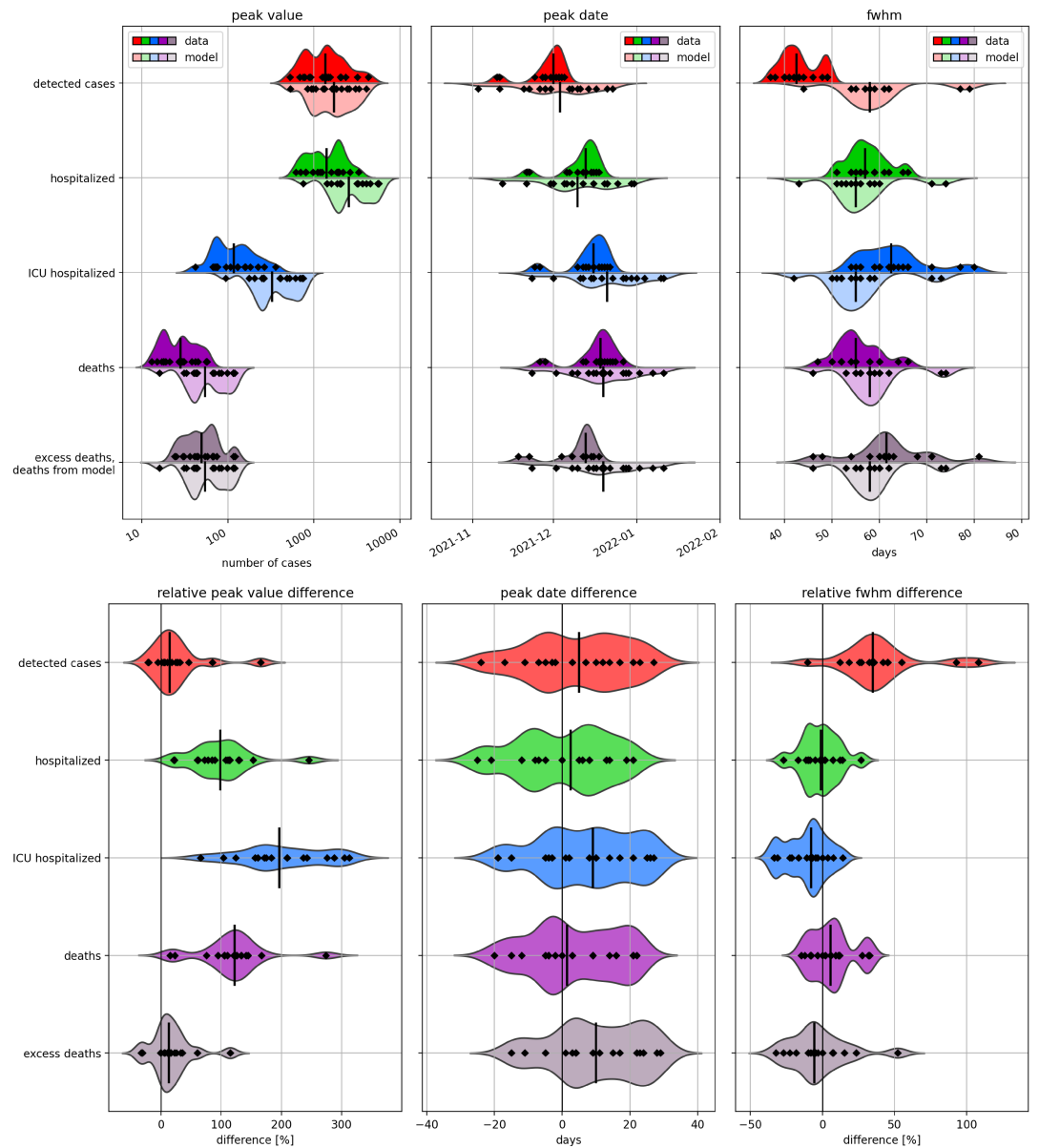


Figure 7. Summary results for the model forecast on a regional level. Each data point refers to one voivodeship. Upper panels present smoothed distributions of peak value, peak date, and FWHM separately for the Ministry of Health data (above horizontal reference lines) and the model forecast data (below the reference lines) for daily new detected cases, occupied hospital beds, occupied ICU beds, and COVID-19 deaths (compared also to excess deaths based on the Eurostat data (Eurostat, 2023a)). Lower panels present smoothed distributions of relative peak value difference, peak date difference, and relative FWHM difference between the model forecast and the official data. The data points are accompanied by median values (vertical black segments).

346 Discussion

347 Mathematical epidemic models play a crucial role in understanding and informing effective mitiga-
 348 tion strategies for disease outbreaks (Brauer, 2008; James et al., 2021; Marshall, 2017; Ferguson
 349 et al., 2020, 2005). This manuscript focuses on validating the epidemic dynamics and assessing the
 350 forecasting accuracy of pDyn, an agent-based model specifically designed to capture and predict
 351 the dynamics of COVID-19 in Poland.

352 The pDyn possesses several key strengths for modeling epidemic dynamics. Firstly, it excels in

353 capturing intricate social networks and contact patterns among individuals, factors with a substan-
354 tial impact on disease transmission. Consequently, it provides valuable insights into the individual-
355 based and network-based mechanisms governing epidemic spread. Secondly, the model's versatil-
356 ity allows it to simulate epidemics at different spatial scales, thanks to its incorporation of geospa-
357 tial data such as population demographics and transportation networks. These features enable
358 the simulation of various intervention strategies, such as quarantine and social distancing, and
359 their impact on epidemic spread. Additionally, pDyn models multiple pathogen variants and cross-
360 immunity, shedding light on the role of variant and vaccine diversity in epidemic dynamics. It also
361 integrates a model for immunity acquisition and waning, enabling the simulation of the effects of
362 vaccination and natural infection.

363 In the study presented in this manuscript, we aimed to achieve three objectives:

- 364 1. We first assessed the model's validity in simulating the dynamics of pathogen variants suc-
365 cession, immunization processes, and the proportion of vaccinated individuals among con-
366 firmed cases.
- 367 2. We then assessed the model's predictive capabilities by examining its performance in fore-
368 casting the dynamics of confirmed cases, hospitalizations, ICU admissions, and deaths during
369 the epidemic wave, focusing on critical metrics like peak timing, peak magnitude, and wave
370 duration.
- 371 3. Lastly, we explored the utility of pDyn in forecasting disease-related dynamics within Poland's
372 highest administrative units using national-level data. This was made possible through the
373 use of a virtual population representing the social and demographic structure of Poland.

374 We summarize our findings and discuss them below.

375 The first aspect we examined to validate the model was the progression of variants. This dy-
376 namic depends on various factors, including variants' properties like cross-immunity and infectiv-
377 ity, as well as the spatiotemporal distribution of initial infections for each variant. It is important
378 to note that pDyn considers cross-immunity, seasonal fluctuations, and regulatory changes based
379 on official data but does not incorporate emerging behavioral changes that could influence the
380 model.

381 Our study revealed that the Delta variant reached prevalence milestones of 25%, 50%, and 75%
382 two, three, and four weeks later, respectively, compared to the GISAID genomic data. Our valida-
383 tion aligns with prior research such as *Eales et al. (2022)* and *Dong et al. (2022)*, which assessed
384 variant succession at the 50% prevalence point. These studies reported prediction errors within
385 one to two weeks, indicating a similar level of accuracy to pDyn, albeit slightly better. However,
386 the superior performance of other models compared to pDyn may be partially attributed to their
387 calibration and validation using the same datasets, whereas pDyn underwent calibration and val-
388 idation using separate datasets. Two other studies solely offered visual comparisons (*Coutinho*
389 *et al., 2021*; *Campbell et al., 2021*). It should also be mentioned that potential selection bias in
390 GISAID estimates for Poland could contribute to observed differences. Nevertheless, it can be con-
391 cluded that our findings demonstrate that pDyn effectively replicates variant succession.

392 Next, we compared our modeling outcomes with the OBSER-CO seroprevalence survey con-
393 ducted by the National Institute of Public Health. Our model's cumulative count of recovered and
394 vaccinated individuals closely aligned with the seroprevalence study's estimates at all four study
395 rounds. However, the estimate for December 2021 was slightly elevated, falling three percent-
396 age points outside the 95% confidence interval. While models akin to ours have been calibrated
397 against seroprevalence data, they have not, to our knowledge, undergone validation against such
398 data (*Kemp et al., 2021*; *Jentsch et al., 2021*).

399 Some data issues can contribute to the uncertainty of our validation. OBSER-CO results esti-
400 mates might be influenced by instability in detecting cases related to the testing during rising and
401 falling epidemic waves (*Rippinger et al., 2021*). Furthermore, the study rounds extended over time,

402 with unevenly distributed testing within each round, while seroprevalence was estimated at spe-
403 cific central time points within each round interval, which could have influenced estimate accuracy.
404 Moreover, the sum of recovered and vaccinated cases derived from the model does not align per-
405 fectly with OBSER-CO seroprevalence statistics based on antibody levels in the trial groups. Despite
406 these reservations, pDyn's representation of immunity in society closely mirrors empirical OBSER-
407 CO studies. Importantly, pDyn is, to our knowledge, the first model to faithfully reflect empirical
408 seroprevalence, rendering it a valuable tool for exploring epidemic dynamics.

409 The proportion of vaccinated detected cases, considered a simulation variable, was compared
410 with surveillance data from the Ministry of Health, using mean absolute error (MAE) as the valida-
411 tion metric. The MAE was smaller for the period before the forecast date (from January 1, 2021, to
412 October 28, 2021) than for the forecast period (from October 29, 2021, to December 31, 2021,),
413 reflecting the inherent uncertainty in predictions. Notably, the maximum absolute error (in the
414 period from January 1, 2021, to December 31, 2021) occurred on October 18, 2021, reaching 14.01
415 percentage points. This peak coincided with low case numbers and high vaccination coverage, con-
416 tributing to the observed variation. It is noteworthy that while the proportion of fully vaccinated
417 individuals among detected cases has been used to assess vaccine effectiveness in empirical stud-
418 ies (*Arashiro et al., 2022*), it has not been commonly employed in epidemic modeling validation.

419 In summary, the pDyn model generated dynamics that generally aligned with epidemiological
420 data, affirming the validity of the model's dynamics of variant succession, immunization, and the
421 emergence of vaccinated individuals among confirmed cases.

422 Our proposed approach to handling uncertainty in generative models, like pDyn, offers added
423 value to the epidemiological modeling domain. ABMs often involve numerous parameters requir-
424 ing calibration, and the available data are insufficient for calibrating each parameter individually.
425 In such cases, part of the model validation process may involve comparing variables that are not
426 direct model outputs but can be derived from the model and compared to existing data before
427 making forecasts—examples include the dynamics of pathogen variant succession, immunization,
428 and the emergence of vaccinated individuals among confirmed cases. This approach aids in testing
429 the validity of processes implemented in the model.

430 In the second phase of our study, we assessed the forecast accuracy for the Delta variant wave
431 at the national level. This assessment encompassed new cases, hospitalizations, ICU admissions,
432 and COVID-19-related deaths, focusing on peak value, peak date, and wave length.

433 The number of new COVID-19 cases, our primary output and reference for model calibration,
434 provided precise forecasts for the peak value, with only a slight deviation of 6.84%. However, other
435 aspects of the forecast exhibited overestimations. Notably, the predicted peak timing experienced
436 a delay of six days, and the prediction of wave length (measured by FWHM) needed to be more
437 accurate for new cases. This discrepancy can be attributed, in part, to the constant detection ratio
438 implemented in our model. However, during the holiday season in December 2021, testing rates
439 and detection ratios likely decreased, resulting in fewer confirmed cases and contributing to lower
440 forecast accuracy.

441 The model predicted a significantly higher number of COVID-19-related general and ICU hospi-
442 talizations than the Ministry of Health reported, with 76% more hospitalizations and 151% more
443 ICU patients. When building the model, we focused on required instead of occupied beds, assum-
444 ing that even if some patients needing hospitalization stayed home, the health system should be
445 prepared. This assumption is a primary source of the discrepancy between the model and data. Ad-
446 ditionally, the model assumes constant hospitalization durations of 10 days for general and seven
447 days for ICU admissions instead of using distributions, and poor data quality related to hospital-
448 ization durations adds uncertainty to estimations.

449 Our analysis revealed dynamically changing case-to-hospitalization and case-to-death ratios
450 throughout the waves. These changes can be attributed to social reluctance towards testing and
451 hospitalization due to difficult hospital conditions. Factors such as lack of family contact, admission
452 challenges, and long queues at testing sites could contribute to this hesitance (*Kołodziej and Pecka,*

453 *2021; Grove et al., 2023; Rewerska-Juško and Rejdak, 2022; Tran et al., 2020; Wong et al., 2022;*
454 *Zheng et al., 2021*). However, the model did not account for psychological and healthcare system
455 overload behavioral effects, which also affected the accuracy of our predictions.

456 Despite these caveats, peak time forecasts for hospitalizations were the most accurate among
457 predicted disease-related states (2 days delay), and the relative wave length difference was best
458 for ICU patients (-1.5%). In summary, the discrepancy between hospitalization and ICU patient data
459 and model results refers to wave magnitude rather than peak or length. This result emphasizes
460 the need to consider the forecast objectives and factors influencing access and utilization of health
461 services when interpreting modeling outcomes, along with data collection challenges, to improve
462 hospitalization nowcasting (*Wu et al., 2021; Wolfram et al., 2023*).

463 In this study, pDyn projected more COVID-19-related deaths than officially reported, aligning
464 better with excess deaths, which capture undetected infections. For instance, *Walkowiak and*
465 *Walkowiak (2022)* found that combined COVID-19-related deaths accounted for 95% of excess
466 deaths among Polish adults over 40. Death forecasts closely matched excess deaths in peak value
467 (5% relative difference) and wave length (3% relative difference). However, the peak date for deaths
468 was the least accurate among all forecasted states, with an 11-day delay. The alignment of death
469 modeling results with actual data is notably influenced by data collection issues, primarily attribut-
470 ing deaths to COVID-19, which is less reliable in Poland than other epidemiological data collected
471 during the pandemic. The model's alignment with excess mortality data in our study supports
472 COVID-19's substantial contribution to overall excess mortality during the pandemic (*Msemburi*
473 *et al., 2023; Wang et al., 2022; Woolf et al., 2020*), particularly in Poland.

474 The pDyn model, grounded in a synthetic society reflecting regional socio-demographic data,
475 explicitly considers regional variations in vaccination, pre-Delta wave NPIs, and the initial regional
476 spread of wild-type infections in Poland. However, its calibration relies on national epidemic data.
477 Our study aimed to evaluate the precision of regional forecasts generated by this model on the
478 voivodeships level.

479 Our findings indicate that, on average, regional forecasts align with national-level ones, with me-
480 dian differences resembling those at the national level. However, prediction quality varies among
481 voivodeships, with Podkarpackie voivodeship emerging as an outlier regarding relative peak value
482 differences for detected cases, occupied hospital beds, and deaths. These substantial differences
483 likely stem from localized variations in social responses to the epidemic and restrictions, under-
484 scoring the need to consider regional social attitudes for better regional forecasting.

485 To improve regional forecasting, incorporating agent features related to behavioral traits, such
486 as trust in medicine and willingness to adhere to NPIs and vaccination, is advisable. Addition-
487 ally, continual monitoring of local conditions and model adaptation to regional specifics enables
488 more accurate predictions. Local models with adaptable parameterization, focusing on the short
489 or medium-term, generally outperform global and long-term models (*Bracher et al., 2022*).

490 Despite the promising results, our study has limitations common to complex ABMs like pDyn,
491 including the challenge of calibrating numerous parameters with limited data. This parameter
492 calibration issue significantly contributes to forecast uncertainty. We attempted to address this by
493 validating the model's parameterization by comparing model dynamics with real-world data, but
494 these challenges persist, introducing inherent uncertainty into our forecasts.

495 Like all epidemiological models, pDyn encounters challenges in predicting unpredictable phe-
496 nomena that can arise during an epidemic, such as pathogen mutations or shifts in social contact
497 patterns, which can substantially influence the epidemic's trajectory. Our model does not include
498 long-term predictions of pathogen evolution or the modeling of socio-behavioral dynamics. In-
499 stead, parameters related to these aspects are introduced post-hoc, often with delays, adding to
500 the overall uncertainty of the model's predictions.

501 To enhance forecast accuracy, developing new features in the future may be necessary. Cur-
502 rently, the model assumes constant durations for health-related states (e.g., hospitalization), while
503 using parameter distributions could improve realism. Simplified modeling of transportation and

504 commuting could be expanded for better representation of local and long-distance transmission.
505 Agent behavior could be refined by introducing behavioral attributes, and contact change calibration
506 would benefit from using external data, like mobility. However, these extensions increase
507 the number of parameters to calibrate, computational complexity and load, as well as introduce
508 inherent uncertainties (e.g., mobility change only proxies contact pattern change).

509 Data availability remains a fundamental limitation of the pDyn model. Several crucial datasets
510 were unavailable at the time of our forecasting, including contact tracing data, the influx of new
511 cases, the number of households in quarantine, and estimated transmissions between household
512 members. Also, much of the data available during the data epidemic was biased and would require
513 modeling (like nowcasting of hospitalization data). In particular, there needed to be more effort
514 in obtaining current and reliable data quickly. These issues underscore the importance of robust
515 and timely epidemic surveillance systems for mathematical modeling of epidemics.

516 Nonetheless, despite limited data availability, the pDyn model provided valuable insights into
517 epidemic processes and demonstrated remarkable forecasting efficiency. It can aid in understand-
518 ing epidemic mechanisms and inform epidemic policy design by enabling the comparison of mul-
519 tiple scenarios.

520 In summary, our study highlights the pDyn model's robust capabilities and potential for provid-
521 ing reliable and insightful forecasts across various aspects of the COVID-19 pandemic. Key findings
522 can be summarized as follows:

- 523 1. *Model Validation:* The generative ABM pDyn employs intricate internal states to incorporate
524 extensive data, allowing for the representation of mechanisms beyond the scope of phe-
525 nomenological models. We validated the model's accuracy in simulating pathogen variant
526 succession, immunization processes, and the proportion of vaccinated individuals among
527 confirmed cases, revealing close alignment with real-world data. Additionally, we introduced
528 an innovative approach to address uncertainty in generative models. This approach involves
529 comparing model-generated variables, which were not targeted initially as outputs, with real-
530 world data, thereby enhancing our ability to analyze patterns.
- 531 2. *Predictive Capabilities:* The meticulous generative description of epidemic spread in pDyn re-
532 sults in impressive predictive performance, encompassing new cases, hospitalizations, ICU
533 admissions, and deaths. Evaluations within the German and Polish COVID-19 Forecast Hub
534 and the European COVID-19 Forecast Hub confirmed these capabilities. In our assessment
535 of predictive capabilities, we focused on peak timing, peak magnitude, and wave duration
536 for confirmed cases, hospitalizations, ICU admissions, and deaths. While peak values were
537 often overestimated, the model consistently captured the dynamics of the Delta wave. Our
538 findings underscore the importance of aligning forecasting interpretation with the challenges
539 related to data collection during epidemics. This highlights the role of informed nowcasting,
540 particularly for data related to infection-related hospitalizations and deaths.
- 541 3. *Regional Forecasting:* pDyn enables detailed epidemic simulations at both national and re-
542 gional levels, providing a granular perspective on disease dynamics. However, forecasting at
543 the regional level using national data has inherent limitations. Our examination of regional
544 forecasting within Poland's administrative units revealed alignment with real-world data, al-
545 though variations were observed, likely influenced by regional behavioral factors.

546 In conclusion, the pDyn model possesses numerous strengths, including its capacity to model
547 complex social networks, simulate epidemics across different spatial scales, and account for pathogen
548 variants and immunity dynamics. Our comprehensive evaluation underscores its reliability in mod-
549 eling COVID-19 dynamics in Poland, providing valuable insights for informing public health decision-
550 making and mitigation strategies.

551 Finally, we propose recommendations for epidemiological ABMs:

- 552 • *Extend Validation:* ABMs should regularly validate their models by comparing internal vari-
553 ables with empirical data. This approach facilitates the validation of emergent epidemiolog-

554 ical dynamics without the need for individual parameter validation, especially in situations
555 where parameter validation is challenging. Additionally, conducting step-by-step validation
556 for specific phenomena, such as reinfections and vaccine efficacy, can provide a deeper un-
557 derstanding of the model's characteristics and increase confidence in the accuracy and ro-
558 bustness of its results.

- 559 • *Monitor Local Changes*: Monitoring local changes in epidemics, including the presence of vari-
560 ants of concern and shifts in seroprevalence, along with behavioral effects of mitigation
561 strategies like vaccination campaigns, lockdowns, and testing, is essential. This practice al-
562 lows for the customization of models and parameters to specific country or regional situa-
563 tions, leading to improved short and medium-term forecasting accuracy.
- 564 • *Enhance Monitoring Systems*: There should be a concerted effort to enhance monitoring sys-
565 tems in two critical dimensions — data quality and data coverage. Institutions responsible
566 for data collection and monitoring should gain a deep understanding of the empirical data
567 requirements for complex models like pDyn. Leveraging the fastest and most accessible data
568 streams can significantly inform and improve modeling efforts.

569 These recommendations aim to strengthen the reliability and effectiveness of epidemiological
570 ABMs, ultimately aiding in better preparedness and decision-making during disease outbreaks.

571 **Materials and methods**

572 **The pDyn model**

573 Our research utilizes pDyn, the detailed epidemiological ABM developed at the Interdisciplinary
574 Center for Mathematical and Computational Modelling at the University of Warsaw, Poland (ICM) (*Niedzielewski*
575 *et al., 2022*). The simulator was optimized for High-Performance Computing environment and runs
576 in the ICM supercomputing facility.

577 The simulator originated as the influenza epidemic model (*Rakowski et al., 2010a*) with follow-
578 ing features implemented: airborne transmission, pathogen characteristics (i.e. transmissibility),
579 self-isolation, social contacts settings (i.e. households, workplaces, schools, universities, public
580 places, long distance travels), SIR states. Subsequently, during the COVID-19 pandemic, it has been
581 expanded with features tailored to represent characteristics of the SARS-CoV-2 infection, to facili-
582 tate the Polish government's infection prevention and control the decision-making process. The fol-
583 lowing new components have been implemented: partial immunity, variants of pathogen/vaccines,
584 quarantine, partial school closure (i.e. age dependent), reactive NPIs, regional NPIs, changing con-
585 tact rates, vaccination, immunity waning, cross-immunity, dark figure, times and transition prob-
586 ability table (i.e. of the disease-related states), age-dependency of time and transition to disease
587 states, new social contact settings (i.e. kindergartens), new disease-related states (i.e. asymp-
588 tomatic, symptomatic, hospitalized pre-ICU, at ICU, not at ICU).

589 To better illustrate the pDyn's scale and complexity, we present a mind map in the *Figure 2* that
590 organizes the model elements in a transparent, modular way. It explicitly depicts the version of the
591 model used in the study. Functions developed by adapting the original version of the simulator to
592 the COVID-19 are marked in the figure by asterisk (*). The detailed description of the pDyn model
593 following the Overview, the Design concepts, and the Details protocol (ODD, (*Grimm et al., 2020*))
594 is publicly available (*Niedzielewski et al., 2022*).

595 The overall *purpose* of the pDyn model is to describe and explain the spatial and temporal
596 dynamics of SARS-CoV-2 spread across Polish society. The model predicts the dynamics of the
597 number and locations of disease-related states of agents in response to specific changes in the
598 properties of the pathogen and the social structure and behaviour.

599 Two types of *entities* are included in the model: agents and contexts. Agents represent mem-
600 bers of the society. Contexts capture interactions between agents; they represent locations at
601 which the agents come in contact, such as households, workplaces, kindergartens, schools, univer-
602 sities or public places. Their geo-localized representations are included in the synthetic society as

603 model input (*Rakowski et al., 2010b*). The synthetic society is based on data provided by the Statis-
604 tics Poland (*Statistics Poland, 2019*) and reflects the state at the beginning of 2019. The *spatial*
605 *resolution* of the contexts is a grid of 1×1 km² (for Poland, it requires 800×800 grid cells). Addition-
606 ally, pDyn models the mobility of agents via random long-distance travels (i.e. when an agent leaves
607 its household for more than a day). Each agent is assigned to one or more contexts (household at
608 least) that it visits daily.

609 Both agents and contexts are characterized by *state variables*. The agent's state variables are as
610 follows: age, list of contexts to which it is assigned (including primary household), disease-related
611 state, presence of symptoms, being on quarantine, travel status, transmission location, and his-
612 tory of immunization events. The context's state variables are as follows: spatial coordinates of a
613 given context, transmission rate in this context, the number of agents in this context, the number
614 of symptomatic infectious agents in this context, and the number of non-symptomatic infectious
615 agents in this context. The *time resolution* in the simulation is one day.

616 The most important *process* of the model is airborne transmission.

617 For a given susceptible agent, for a given day of the simulation, and a given variant of the virus,
618 the probability of becoming infected by that variant on the following day is computed based on
619 three factors: (1) the infectivity parameter specific to the variant, (2) the infectivity of the contexts
620 visited during the day which we define as the fraction of infectious agents infected with the con-
621 sidered variant in that context, (3) the weights of the daily visited contexts which represent the
622 contact rate of the agents in that context.

623 Thus, the probability of each susceptible agent getting infected on the next day of the simu-
624 lation is a function of the *disease-related states* of all agents with whom it has been in contact in
625 contexts during the current day (*Niedziewski et al., 2022*). Immediately after the recovery or af-
626 ter taking a vaccine, the agent is immune to the infection variant of the pathogen, but the level
627 of immunity wanes over time. The level of immunity calculated on a given day of the simulation
628 modifies the probability of infection with the variant. In addition, recovery from infection with a
629 particular variant of the virus generates a certain level of cross-immunity to other variants. Fur-
630 thermore, the context weights are adjusted using *multipliers* in time to represent the changes in
631 the contact rates (i.e., the number of contacts made divided by the number of contact opportuni-
632 ties) due to behavioural reactions to the epidemic, both spontaneous or in response to the control
633 measures.

634 The model of possible *disease-related states* in pDyn expands the SEIR (Susceptible, Exposed, In-
635 fected, Recovered) compartmental model (*Li and Muldowney, 1995*). An agent can find itself in one
636 of the following disease-related states: susceptible, latent, asymptomatic, symptomatic, hospital-
637 ized outside the ICU, hospitalized before ICU, hospitalized at ICU, dead, or recovered state. These
638 disease-related states form an ordered graph that defines possible courses of infection (*Figure 8*).
639 At each branching, probability parameters have been introduced to control the likelihood of the
640 specific transitions between states (specific to the pathogen variant).

641 In addition, the duration of each state is defined. The transition probabilities and the duration of
642 states depend on agent's age. It is assumed that both the asymptomatic and symptomatic states
643 are infectious and that infectivity in the symptomatic state is higher than in the asymptomatic
644 one (*Sayampanathan et al., 2021; Han et al., 2020; Zhao et al., 2020*). On the other hand, there is
645 a possibility for an agent in a symptomatic state to undergo self-isolation or quarantine, meaning
646 the agent withdraws from all contexts except for the household. The probability and duration
647 parameters were selected based on several studies (*Gold et al., 2020; Carrillo-Vega et al., 2020;*
648 *Petrilli et al., 2020; Ko et al., 2021; Twohig et al., 2022*) and their values implemented in the present
649 simulation are presented in *Appendix 3*.

650 In the pDyn, the number of infected agents includes both detected and undetected cases. Un-
651 detected cases impact various aspects of pandemic dynamic such as the true disease spread, the
652 number of immunised individuals, numbers of hospitalized cases and deaths. The model intro-
653 duces a *dark figure* representing the number of undetected cases, generating outputs for both real

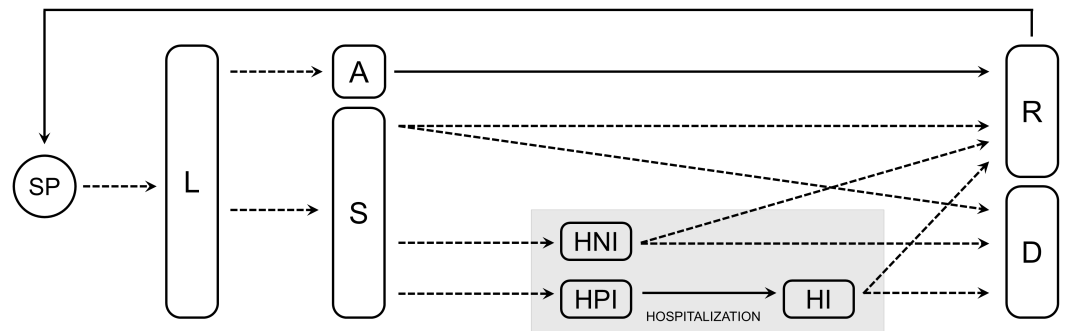


Figure 8. The possible paths through disease-related states in the pDyn model. The state abbreviations stand for SP — susceptible, L — latent, A — asymptomatic, S — symptomatic, HPI — hospitalized, pre-ICU, HI — hospitalized, at ICU, HNI — hospitalized, not at ICU, D — dead, R — recovered. In addition, there are three surefire paths (with transition probability equal to 1; marked with solid arrows) regardless of the agent's age.

654 cases (detected and undetected) and detected cases. The dark figure changes over time and is
 655 estimated by considering factors such as the ratio of non-symptomatic to symptomatic cases, test-
 656 ing strategies, test types, test numbers, contact tracing, public trust, and seroprevalence screening
 657 studies (*National Institute of Public Health, 2023*).

658 The pDyn model simulate vaccination programs, considering factors like geographical distribu-
 659 tion, agent's age, and the number of vaccines administered. However, the presented simulation is
 660 agnostic to the type of vaccination, treating boost vaccinations the same as first doses, and not dif-
 661 ferentiating between various vaccines. The model offers fine-tuned control of vaccination, allowing
 662 for region-specific and age-based vaccination strategies with limited supply considerations based
 663 on data provided by Polish government under the license defined in a Non-Disclosure Agreement.

664 The pDyn explicitly addresses the cross-immunity phenomenon. The model assumes that the
 665 agent is immune to the infection variant immediately after recovery or after taking a vaccine, albeit
 666 the immunity level is waning over time. The decline in the immunity level is described in the func-
 667 tion of elapsed time since recovery and can take values between 0 and 1 (*Figure 1 in Appendix 3*).
 668 The immunity level of an agent computed on a given day of the simulation modifies the proba-
 669 bility of infection with the variant subject to immunity. Moreover, we model the phenomenon of
 670 cross-immunity by assuming that recovery from an infection with a specific virus variant generates
 671 some immunity level to other variants. The parameters related to (cross-)immunity were estimated
 672 from (*Scobie et al., 2021*) and presented in *Appendix 3*.

673 The pDyn allows to model risk exposure changes, whether seasonal (e.g. school closure during
 674 holidays) or behavioural (e.g. in response to NPIs, e.g., online schooling), by switching off or tuning
 675 contexts, using context weight *multipliers*. To our best knowledge, no systematic studies of contact
 676 rates changes were carried out during the COVID-19 epidemic in Poland. Instead, the models use
 677 intermediate (e.g., estimates based on measurements of the use of mobile networks) or partial
 678 (e.g., social mixing surveys) measures. In pDyn, the initial contacting rates were adopted from
 679 original influenza model (*Rakowski et al., 2010a*). Changes in contact rates during the outbreak
 680 and subsequent restrictions were implemented through multipliers.

681 In order to model changes in the contact rate for a particular context, we utilized the calibra-
 682 tion experiments method, except for educational units, for which these multipliers were estimated
 683 based on the proportion of pupils attending them. Multipliers for the households, workplaces, and
 684 public places were adjusted with an assessment of the change in contact rates (based on changes
 685 in the number of people and their compliance with social distancing measures in a given context).
 686 The calibration experiments were executed in the following way: first we established the optimistic
 687 and pessimistic contact rate scenarios by assessing the minimum and maximum values of multipli-
 688 ers (such as low vs. high face mask use compliance). For example, on March 12, 2020, the mandate

689 of remote work and social distancing at the workplace was introduced, therefore we reduced the
690 value of the workplace context multiplier from 1 to 0.5 in the optimistic scenario and to 0.8 in the
691 pessimistic scenario. Then, we tested several multiplier values in the selected range to compare
692 the results with the actual data of the identified cases from 14 days after the introduced change
693 and adjusted the value of multipliers as necessary. In order to determine the best set of multipliers,
694 the Fréchet distance between the number of confirmed cases predicted by the model and the real-
695 world data was minimized. The final list of all context multipliers is presented in the **Appendix 3**.

696 Regional diversity of the predicted epidemic dynamic on voivodship level is only due to a spatial
697 structure of the synthetic society, some regional differentiation of weight multipliers motivated by
698 regional NPIs in force before the Delta wave as well as location of infected agents spatially placed
699 at the simulation date.

700 **Input data and calibration**

701 In pDyn, the infection spread is simulated on a synthetic representation of Polish society compris-
702 ing about 38 million agents representing Poland's population in 2019, simulated based on Statis-
703 tics Poland data, both publicly (*Statistics Poland, 2019; Rakowski et al., 2010b*) and not publicly
704 available. Non-public data was provided under the license defined in a Non-Disclosure Agreement
705 and can be made available with the permission of the data provider. The spread of epidemics
706 and individual virus variants begins with initial infections, which serve as an initial condition of the
707 simulation. Data on the date and location of the initial infections have provided by the Polish Min-
708 istry of Health (please see **Appendix 4**, containing data sources). Initial parameters are loaded to-
709 gether with the synthetic society at the beginning of the simulation. The initial parameters include
710 pathogen properties (infectivity, probabilities and times of disease-related states per variant), the
711 proportion of undetected cases, quarantine probability, cross-immunity and immunity waning pa-
712 rameters, and context weights, and their multipliers.

713 Two parameters, namely the basic pathogen variant infectivity (α) and the fraction of not self-
714 isolating symptomatic agents (f) were fitted in the model calibration process using Bayesian opti-
715 mization (*Shahriari et al., 2016*) to the real-world number of confirmed cases provided initially by
716 Michał Rogalski and then by the Polish Ministry of Health. The remaining parameters were taken
717 from the literature (as indicated in the model description) or estimated based on calibration exper-
718 iments, such as those described for modeling changes in the contact rates for different contexts
719 (*multipliers*). Similarly to setting optimistic and pessimistic scenarios for multipliers, we dealt with
720 the uncertainty for the remaining model parameters by setting specific prediction intervals based
721 on optimistic and pessimistic scenarios.

722 In stochastic models, such prediction intervals may arise from several interrelated sources.
723 Firstly, it can be derived from a number of simulations carried out with alternating seeds of the
724 pseudo-random number generator. Secondly, it can be derived from several simulations with al-
725 ternating input parameter values taken from appropriate distributions. Thirdly, the assumed or
726 prepared initial state of the system, e.g. the immunisation of the population, might strongly af-
727 fect the outcome values of the simulation. Finally, the result of time-dependent curve prediction
728 intervals for each time point forms a confidence interval.

729 As a result, broad prediction intervals can be obtained in the simulations of highly non-linear
730 systems, where the small random change of input parameters might result in a significant out-
731 put change. However, the broad prediction intervals appear when input parameters are delivered
732 with a broad range of possible values or where the system's initial state features are largely un-
733 known. In our case, the nonlinearity of the model is limited, and the main source of the output
734 uncertainty comes from the uncertainty of various parameter values and the system's initial state.
735 In such a situation, apart from computing the confidence corridors resulting from the randomness
736 of the process, the two extreme scenarios have been formulated: the lowest (optimistic) and the
737 highest (pessimistic), regarding possible but still realistic values of parameters and initial states of
738 the system. The two scenarios determine the prediction interval for our forecast. The contrast in

739 uncertainty coming from different sources (random seed vs two scenarios) is illustrated for the
740 simulation described in **Appendix 5**.

741 **Simulation setup**

742 **Hardware**

743 Computations are performed on Cray XC40 (Okeanos) that is part of ICM computing infrastructure.
744 System is composed of 1084 computing nodes. Each node has 24 Intel Xeon E5-2690 v3 CPU cores
745 with a 2-way Hyper Threading (HT) with 2.6 GHz clock frequency. Single simulation on single nodes
746 takes around 2 hours (time depends on parameters configuration).

747 **Model calibration**

748 The simulation used in this study was conducted on October 28, 2021. In order to account for the
749 uncertainty, we have formulated pessimistic and optimistic scenarios differing in the dark figure
750 parameter (see **Appendix 5**) that was estimated using seroprevalence and registered cases data.
751 The pessimistic scenario proved to yield a more accurate prediction of the Delta-variant wave than
752 the optimistic scenario. Therefore, all presented results come from the pessimistic scenario).

753 **Testing validity of the model dynamics**

754 It should be noted at the beginning that when testing the validity of the model, we compared the
755 real-world data (other than those to which we calibrated the model) to our model estimates to
756 evaluate whether the pDyn reproduced the dynamics of the epidemic accurately up to the time
757 of simulation (i.e., October 28 2021). When testing the accuracy of the pDyn's predictions, we
758 retrospectively compared the results obtained in the simulation with real-world data acquired after
759 the simulation date to evaluate pDyn as a tool for predicting the future epidemic spread.

760 We tested the validity of the epidemic dynamics implemented in the model by comparing our
761 simulations with real-world data regarding the dominating SARS-CoV-2 variant, immunization level
762 in the population, and the fraction of vaccinated amongst detected cases.

763 The emergence of the variants of pathogen in the real world is monitored, and data are collected
764 and accessible via Global Initiative on Sharing Avian Influenza Data (GISAID) portal (*Khare et al.,*
765 **2021**). The distribution of SARS-CoV-2 variants in our model was validated by comparison with the
766 genomic data from the GISAID. Before the day of our simulation, three dominant variants have
767 been detected in Poland (namely, the wild type, Alpha, and Delta). To account for the possible low
768 representativeness of the GISAID samples available for Poland, we assessed whether the curves
769 representing the temporal succession of the wild type, Alpha and Delta variants obtained from
770 our model mirrors the analogous "succession curves" obtained from GISAID by comparing the
771 time convergence of reaching 25%, 50%, and 75% prevalence for each variant.

772 Similarly, to establish the immunization level (the fraction of agents who have been vaccinated
773 or have undergone disease and are still immune), we compared the model results with the results
774 of a nation-wide seroprevalence survey of adults aged 19 years and older (named OBSER-CO) run
775 by the National Institute for Public Health in Poland (*National Institute of Public Health, 2021,*
776 **2023**). This data was collected in four rounds (I round: 29 March to 14 May 2021, II round: 27 July
777 to 10 September 2021, III round: 16 November to 23 December 2021, IV round: 14 March to 4 May
778 2022) alongside with 95% confidence intervals for each estimate. The OBSER-CO seroprevalence
779 estimates were used to approximate the validity of pDyn's predictions of the cumulative sum of
780 recovered and vaccinated agents. As only the adult population was studied in the OBSER-CO study,
781 data of agents younger than 19 years were not included in **Figure 4**.

782 Lastly, using the Ministry of Health data on the age, time, and location distribution of vaccina-
783 tions, pDyn model computed the fraction of vaccinated among the detected cases. We tested the
784 validity of this estimate by comparing it with the Ministry of Health's estimate of the fraction of
785 vaccinated detected cases in the population using mean absolute error (MAE) method.

786 Testing the forecast accuracy

787 In order to evaluate the performance of our model and the accuracy of the simulation in repro-
788 ducing the COVID-19 dynamics, we compared its results to real-world data (from the Ministry of
789 Health [quote]) using three key measures of discrepancy: (1) the difference in peak date, (2) the
790 difference in peak value, and (3) the difference in wave length.

791 To calculate the differences, we first characterized the peaks of the COVID-19 pandemic by
792 fitting a parameterized analytical function to the data indicating the occurrence of a wave. As
793 the logistic curve is typically used to approximate a cumulative number of infected cases in epi-
794 demics (*Lee et al., 2020; Postnikov, 2020*), its derivative, known as the logistic distribution, is a
795 natural choice for a description of daily cases. The logistic distribution is parameterized by three
796 quantities, which can be matched to our measures: (1) the mean (peak data, the central point of
797 the wave peak), (2) the height (peak value), and (3) the width (wave length). The latter was adapted
798 for our analysis as a full width at half-maximum (FWHM) (*Bonifazi et al., 2021*). In *Appendix 6* we
799 provided a mathematical formula for calculating FWHM, as well as details and examples of the
800 fitting procedure.

801 This analysis was applied to the peaks of new confirmed cases, COVID-19-related deaths, hos-
802 pitalized patients, and ICU patients, both at the national and regional levels, and both for model
803 results and real-world data. Although within the real-world data the Delta wave peaks are usually
804 partially overlapped with arising Omicron wave peaks (not taken into account in the forecast), a
805 sum of two logistic distributions of individual parameters were fitted in this case, and only the first
806 peak of Delta wave was taken for further analysis. The same method was employed to test the ac-
807 curacy of predictions at the level of voivodships, which are the basic administrative units in Poland
808 where epidemic data is collected and potential NPIs are introduced.

809 Acknowledgments

810 This research was carried out with the support of the Interdisciplinary Centre for Mathematical
811 and Computational Modelling University of Warsaw (ICM UW) under computational allocation no
812 GS80-31.

813 Data and Code Availability

814 The research presented in this paper is based on both publicly available data and data obtained
815 through an agreement that includes a non-disclosure agreement (NDA). The sources of the data are
816 specified in the Supplementary materials section "S2 Data sources". We have taken all necessary
817 measures to ensure the protection and confidentiality of the data used in this study. We recognize
818 the importance of data sharing for scientific progress and are committed to making our data sets
819 available to other researchers upon request, while adhering to any constraints imposed by the
820 NDA.

821 All publicly available data used in this article is available in the public repository from the link:
822 <https://doi.org/10.18150/8XITKG> The code used in this research is available at [https://git.icm.edu.pl/
823 covid19/1127](https://git.icm.edu.pl/covid19/1127) under Apache License 2.0.

824 References

- 825 **Adamik B**, Bawiec M, Bezborodov V, Bock W, Bodych M, Burgard JP, Götz T, Krueger T, Migalska A, Pabjan
826 B, Ożański T, Rafajłowicz E, Rafajłowicz W, Skubalska-Rafajłowicz E, Ryfczyńska S, Szczurek E, Szymański P,
827 Mitigation and herd immunity strategy for COVID-19 is likely to fail; 2020. doi: [10.1101/2020.03.25.20043109](https://doi.org/10.1101/2020.03.25.20043109).
828 Preprint at <https://www.medrxiv.org/content/10.1101/2020.03.25.20043109v2>.
- 829 **Arashiro T**, Arima Y, Muraoka H, Sato A, Oba K, Uehara Y, Arioka H, Yanai H, Kuramochi J, Ihara G, Chubachi K,
830 Yanagisawa N, Nagura Y, Kato Y, Ueda A, Numata A, Kato H, Ishii K, Ooki T, Oka H, et al. Coronavirus Disease
831 19 (COVID-19) Vaccine Effectiveness Against Symptomatic Severe Acute Respiratory Syndrome Coronavirus
832 2 (SARS-CoV-2) Infection During Delta-Dominant and Omicron-Dominant Periods in Japan: A Multicenter
833 Prospective Case-control Study (Factors Associated with SARS-CoV-2 Infection and the Effectiveness of COVID-
834 19 Vaccines Study). *Clinical Infectious Diseases*. 2022; 76(3). doi: [10.1093/cid/ciac635](https://doi.org/10.1093/cid/ciac635).

- 835 **Banks DL**, Hooten MB. Statistical Challenges in Agent-Based Modeling. *The American Statistician*. 2021;
836 75(3):235–242. doi: [10.1080/00031305.2021.1900914](https://doi.org/10.1080/00031305.2021.1900914).
- 837 **Bicher M**, Rippinger C, Brunmeir D, Urach C, Zechmeister M, Popper N. Agent-Based SARS-CoV-2 simulation
838 model. Model specification. dwh GmbH - TU Wien; 2023. Report at [https://www.dwh.at/en/projects/covid-19/
839 Covid19_Model-20230322.pdf](https://www.dwh.at/en/projects/covid-19/Covid19_Model-20230322.pdf).
- 840 **Bicher M**, Urach C, Popper N. Gepoc ABM: A Generic agent-based population model for Austria. In: *2018 Winter
841 Simulation Conference (WSC)*; 2018. p. 2656–2667. <https://ieeexplore.ieee.org/abstract/document/8632170>, doi:
842 [10.1109/WSC.2018.8632170](https://doi.org/10.1109/WSC.2018.8632170).
- 843 **Bonifazi G**, Lista L, Menasce D, Mezzetto M, Pedrini D, Spighi R, Zoccoli A. A study on the possible merits of using
844 symptomatic cases to trace the development of the COVID-19 pandemic. *The European Physical Journal Plus*.
845 2021; 136(5):481. doi: [10.1140/epjp/s13360-021-01448-2](https://doi.org/10.1140/epjp/s13360-021-01448-2).
- 846 **Bouchnita A**, Jebrane A. A Hybrid Multi-Scale Model of COVID-19 Transmission Dynamics to Assess the Po-
847 tential of Non-Pharmaceutical Interventions. *Chaos, Solitons, & Fractals*. 2020; 138:109941. [https://www.
848 sciencedirect.com/science/article/pii/S0960077920303404](https://www.sciencedirect.com/science/article/pii/S0960077920303404), doi: [10.1016/j.chaos.2020.109941](https://doi.org/10.1016/j.chaos.2020.109941).
- 849 **Bracher J**, Wolfram D, Deuschel J, G3rgen K, Ketterer JL, Ullrich A, Abbott S, Barbarossa MV, Bertsimas D, Bhatia
850 S, Bodych M, Bosse NI, Burgard JP, Castro L, Fairchild G, Fuhrmann J, Funk S, Gogolewski K, Gu Q, Heyder S,
851 et al. A pre-registered short-term forecasting study of COVID-19 in Germany and Poland during the second
852 wave. *Nature Communications*. 2021; 12(1):5173. doi: [10.1038/s41467-021-25207-0](https://doi.org/10.1038/s41467-021-25207-0).
- 853 **Bracher J**, Wolfram D, Deuschel J, G3rgen K, Ketterer JL, Ullrich A, Abbott S, Barbarossa MV, Bertsimas D, Bhatia
854 S, Bodych M, Bosse NI, Burgard JP, Castro L, Fairchild G, Fiedler J, Fuhrmann J, Funk S, Gambin A, Gogolewski
855 K, et al. National and subnational short-term forecasting of COVID-19 in Germany and Poland during early
856 2021. *Communications Medicine*. 2022; 2(1):136. doi: [10.1038/s43856-022-00191-8](https://doi.org/10.1038/s43856-022-00191-8).
- 857 **Brauer F**. Compartmental Models in Epidemiology. In: Brauer F, van den Driessche P, Wu J, editors. *Mathemat-
858 ical Epidemiology*, vol. 1945 Berlin: Springer; 2008.p. 19–79. doi: [10.1007/978-3-540-78911-6_2](https://doi.org/10.1007/978-3-540-78911-6_2).
- 859 **Campbell F**, Archer B, Laurenson-Schafer H, Jinnai Y, Konings F, Batra N, Pavlin B, Vandemaeele K, Van Kerkhove
860 MD, Jombart T, Morgan O, le Polain de Waroux O. Increased transmissibility and global spread of
861 SARS-CoV-2 variants of concern as at June 2021. *Eurosurveillance*. 2021; 26(24). doi: [10.2807/1560-
862 7917.ES.2021.26.24.2100509](https://doi.org/10.2807/1560-7917.ES.2021.26.24.2100509).
- 863 **Carrillo-Vega MF**, Salinas-Escudero G, Garc3a-Pe3a C, Guti3rrez-Robledo LM, Parra-Rodr3guez L. Early estima-
864 tion of the risk factors for hospitalization and mortality by COVID-19 in Mexico. *PLOS ONE*. 2020; 15(9). doi:
865 [10.1371/journal.pone.0238905](https://doi.org/10.1371/journal.pone.0238905).
- 866 **Coutinho RM**, Marquitti FMD, Ferreira LS, Borges ME, da Silva RLP, Canton O, Portella TP, Poloni S, Franco C,
867 Plucinski MM, Lessa FC, da Silva AAM, Kraenkel RA, de Sousa Mascena Veras MA, Prado PI. Model-based
868 estimation of transmissibility and reinfection of SARS-CoV-2 P.1 variant. *Communications Medicine*. 2021;
869 1(1):1–8. doi: [10.1038/s43856-021-00048-6](https://doi.org/10.1038/s43856-021-00048-6).
- 870 **Delussu F**, Tizzoni M, Gauvin L. Evidence of pandemic fatigue associated with stricter tiered COVID-19 restric-
871 tions. *PLOS Digital Health*. 2022; 1(5). doi: [10.1371/journal.pdig.0000035](https://doi.org/10.1371/journal.pdig.0000035).
- 872 **Dilaver O**, Gilbert N. Unpacking a Black Box: A Conceptual Anatomy Framework for Agent-Based Social Simu-
873 lation Models. *Journal of Artificial Societies and Social Simulation*. 2023; 26(1):4. doi: [10.18564/jasss.4998](https://doi.org/10.18564/jasss.4998).
- 874 **Dong R**, Hu T, Zhang Y, Li Y, Zhou XH. Assessing the Transmissibility of the New SARS-CoV-2 Variants: From
875 Delta to Omicron. *Vaccines*. 2022; 10(4):496. doi: [10.3390/vaccines10040496](https://doi.org/10.3390/vaccines10040496).
- 876 **Duszyński J**, Afelt A, Kossowska M, Ochab-Marcinek A, Owczuk R, Paczos W, Plater-Zyberk A, Pyrc K, Rosińska M,
877 Rychard A, Smiatacz T. Kroniki pandemii lata 2020–2021 [Chronicles of the 2020–2021 pandemic]. *Academia —
878 Magazyn Polskiej Akademii Nauk*. 2021; 4(68):1–118. doi: [10.24425/academiaPAN.2021.140621](https://doi.org/10.24425/academiaPAN.2021.140621).
- 879 **Eales O**, de Oliveira Martins L, Page AJ, Wang H, Bodinier B, Tang D, Haw D, Jonnerby J, Atchison C, Ashby D,
880 Barclay W, Taylor G, Cooke G, Ward H, Darzi A, Riley S, Elliott P, Donnelly CA, Chadeau-Hyam M. Dynamics
881 of competing SARS-CoV-2 variants during the Omicron epidemic in England. *Nature Communications*. 2022;
882 13(1):4375. doi: [10.1038/s41467-022-32096-4](https://doi.org/10.1038/s41467-022-32096-4).
- 883 **Elveback LR**, Fox JP, Ackerman E, Langworthy A, Boyd M, Gatewood L. An influenza simulation model for
884 immunization studies. *American Journal of Epidemiology*. 1976; 103(2):152–165. doi: [10.1093/oxfordjour-
885 nals.aje.a112213](https://doi.org/10.1093/oxfordjournals.aje.a112213).

- 886 **Epidemiological Model Team – ICM UW**, COVID-19 w Polsce. RepOD; 2023. <https://doi.org/10.18150/PXSBZM>,
887 doi: 10.18150/PXSBZM.
- 888 **Epstein JM**. Agent-based computational models and generative social science. *Complexity*. 1999; 4(5):41–60.
889 doi: 10.1002/(SICI)1099-0526(199905/06)4:5<41::AID-CPLX9>3.0.CO;2-F.
- 890 **Eurostat**, Deaths by week and sex; 2023. Data at [https://ec.europa.eu/eurostat/databrowser/product/view/
891 DEMO_R_MWK_TS?lang=en](https://ec.europa.eu/eurostat/databrowser/product/view/DEMO_R_MWK_TS?lang=en).
- 892 **Eurostat**, Excess mortality - statistics; 2023. Available from [https://ec.europa.eu/eurostat/statistics-explained/
893 index.php?title=Excess_mortality_-_statistics](https://ec.europa.eu/eurostat/statistics-explained/index.php?title=Excess_mortality_-_statistics).
- 894 **Fazio M**, Pluchino A, Inturri G, Le Pira M, Giuffrida N, Ignaccolo M. Exploring the Impact of Mobil-
895 ity Restrictions on the COVID-19 Spreading through an Agent-Based Approach. *Journal of Transport
896 & Health*. 2022; 25:101373. <https://www.sciencedirect.com/science/article/pii/S2214140522000457>, doi:
897 10.1016/j.jth.2022.101373.
- 898 **Ferguson N**, Laydon D, Nedjati Gilani G, Imai N, Ainslie K, Baguelin M, Bhatia S, Boonyasiri A, Cucunuba Perez
899 Z, Cuomo-Dannenburg G, Dighe A, Dorigatti I, Fu H, Gaythorpe K, Green W, Hamlet A, Hinsley W, Okell L,
900 Van Elsland S, Thompson H, et al., Report 9: Impact of non-pharmaceutical interventions (NPIs) to reduce
901 COVID19 mortality and healthcare demand. Imperial College London; 2020. doi: 10.25561/77482. Report at
902 <https://doi.org/10.25561/77482>.
- 903 **Ferguson NM**, Cummings DAT, Cauchemez S, Fraser C, Riley S, Meeyai A, Iamsirithaworn S, Burke DS. Strategies
904 for containing an emerging influenza pandemic in Southeast Asia. *Nature*. 2005; 437(7056):209–214. doi:
905 10.1038/nature04017.
- 906 **Fox JP**, Elveback L, Scott W, Gatewood L, Ackerman E. Herd Immunity: Basic concept and relevance to public
907 health immunization practices. *American Journal of Epidemiology*. 1971; 94(3):179–189. doi: 10.1093/ox-
908 fordjournals.aje.a121310.
- 909 **Frias-Martinez E**, Williamson G, Frias-Martinez V. An Agent-Based Model of Epidemic Spread Using Human
910 Mobility and Social Network Information. In: *2011 IEEE Third International Conference on Privacy, Security, Risk
911 and Trust and 2011 IEEE Third International Conference on Social Computing* Boston, MA: IEEE; 2011. p. 57–64.
912 doi: 10.1109/PASSAT/SocialCom.2011.142, preprint at <https://doi.org/10.1109/PASSAT/SocialCom.2011.142>.
- 913 **Giacopelli G**. A Full-Scale Agent-Based Model to Hypothetically Explore the Impact of Lockdown, Social Dis-
914 tancing, and Vaccination During the COVID-19 Pandemic in Lombardy, Italy: Model Development. *JMIRx
915 Med*. 2021; 2(3):e24630. <https://xmed.jmir.org/2021/3/e24630>, doi: 10.2196/24630.
- 916 **Gold JAW**, Wong KK, Szablewski CM, Patel PR, Rossow J, da Silva J, Natarajan P, Morris SB, Fanfair RN, Rogers-
917 Brown J, Bruce BB, Browning SD, Hernandez-Romieu AC, Furukawa NW, Kang M, Evans ME, Oosmanally
918 N, Tobin-D'Angelo M, Drenzek C, Murphy DJ, et al. Characteristics and Clinical Outcomes of Adult Patients
919 Hospitalized with COVID-19 — Georgia, March 2020. *MMWR Morbidity and Mortality Weekly Report*. 2020;
920 69(18):545–550. doi: 10.15585/mmwr.mm6918e1.
- 921 **Grimm V**, Railsback SF, Vincenot CE, Berger U, Gallagher C, DeAngelis DL, Edmonds B, Ge J, Giske J, Groeneveld
922 J, Johnston ASA, Milles A, Nabe-Nielsen J, Polhill JG, Radchuk V, Rohwäder MS, Stillman RA, Thiele JC, Ayllón D.
923 The ODD Protocol for Describing Agent-Based and Other Simulation Models: A Second Update to Improve
924 Clarity, Replication, and Structural Realism. *Journal of Artificial Societies and Social Simulation*. 2020; 23(2):7.
925 doi: 10.18564/jasss.4259.
- 926 **Grove C**, Marinucci A, Montagni I. Australian Youth Resilience and Help-Seeking during COVID-19: A Cross-
927 Sectional Study. *Behavioral Sciences*. 2023; 13(2):121. doi: 10.3390/bs13020121.
- 928 **Haischer MH**, Beilfuss R, Hart MR, Opielinski L, Wrucke D, Zirgaitis G, Uhrich TD, Hunter SK. Who is wearing
929 a mask? Gender-, age-, and address-related differences during the COVID-19 pandemic. *PLOS ONE*. 2020;
930 15(10). doi: 10.1371/journal.pone.0240785.
- 931 **Han D**, Li R, Han Y, Zhang R, Li J. COVID-19: Insight into the asymptomatic SARS-COV-2 infection and transmis-
932 sion. *International Journal of Biological Sciences*. 2020; 16(15):2803–2811. doi: 10.7150/ijbs.48991.
- 933 **Hoertel N**, Blachier M, Blanco C, Olfson M, Massetti M, Rico MS, Limosin F, Leleu H. A Stochastic Agent-Based
934 Model of the SARS-CoV-2 Epidemic in France. *Nature Medicine*. 2020; 26(9):1417–1421. [https://www.nature.
935 com/articles/s41591-020-1001-6](https://www.nature.com/articles/s41591-020-1001-6), doi: 10.1038/s41591-020-1001-6.

- 936 **James LP**, Salomon JA, Buckee CO, Menzies NA. The Use and Misuse of Mathematical Modeling for Infectious
937 Disease Policymaking: Lessons for the COVID-19 Pandemic. *Medical Decision Making*. 2021; 41(4):379–385.
938 doi: 10.1177/0272989X21990391.
- 939 **Jentsch PC**, Anand M, Bauch CT. Prioritising COVID-19 vaccination in changing social and epidemiological
940 landscapes: A mathematical modelling study. *The Lancet Infectious Diseases*. 2021; 21(8):1097–1106. doi:
941 10.1016/S1473-3099(21)00057-8.
- 942 **Kemp F**, Proverbio D, Aalto A, Mombaerts L, Fouquier d’Hérouël A, Husch A, Ley C, Gonçalves J, Skupin A, Magni
943 S. Modelling COVID-19 dynamics and potential for herd immunity by vaccination in Austria, Luxembourg
944 and Sweden. *Journal of Theoretical Biology*. 2021; 530:110874. doi: 10.1016/j.jtbi.2021.110874.
- 945 **Khare S**, Gurry C, Freitas L, B Schultz M, Bach G, Diallo A, Akite N, Ho J, TC Lee R, Yeo W, Core Curation Team
946 G, Maurer-Stroh S, GISAID Global Data Science Initiative (GISAID), Munich, Germany, Bioinformatics Insti-
947 tute, Agency for Science Technology and Research, Singapore, Oswaldo Cruz Foundation (FIOCRUZ), Rio
948 de Janeiro, Brazil, Institut Pasteur de Dakar, Dakar, Senegal, National Institutes of Biotechnology Malaysia,
949 Selangor, Malaysia, Smorodintsev Research Institute of Influenza, St Petersburg, Russia, Genome Institute
950 of Singapore, Agency for Science Technology and Research, Singapore, China National GeneBank, Shen-
951 zhen, China, et al. GISAID’s Role in Pandemic Response. *China CDC Weekly*. 2021; 3(49):1049–1051. doi:
952 10.46234/ccdcw2021.255.
- 953 **Ko JY**, Danielson ML, Town M, Derado G, Greenlund KJ, Kirley PD, Alden NB, Yousey-Hindes K, Anderson EJ, Ryan
954 PA, Kim S, Lynfield R, Torres SM, Barney GR, Bennett NM, Sutton M, Talbot HK, Hill M, Hall AJ, Fry AM, et al.
955 Risk Factors for Coronavirus Disease 2019 (COVID-19)–Associated Hospitalization: COVID-19–Associated Hos-
956 pitalization Surveillance Network and Behavioral Risk Factor Surveillance System. *Clinical Infectious Diseases*.
957 2021; 72(11). doi: 10.1093/cid/ciaa1419.
- 958 **Kołodziej B**, Pecka I, Trudna sytuacja w szpitalach. Wstrzymane przyjęcia, coraz mniej wol-
959 nych łóżek [Difficult situation in hospitals. Suspended admissions, fewer and fewer free
960 beds]; 2021. Available from [https://www.medonet.pl/koronawirus/koronawirus-w-polsce,
961 koronawirus--brakuje-lozek-i-lekarzy--czwarta-fala-uderzyla-w-szpitala,artykul,58144898.html](https://www.medonet.pl/koronawirus/koronawirus-w-polsce,koronawirus--brakuje-lozek-i-lekarzy--czwarta-fala-uderzyla-w-szpitala,artykul,58144898.html).
- 962 **Lee SY**, Lei B, Mallick B. Estimation of COVID-19 spread curves integrating global data and borrowing informa-
963 tion. *PLOS ONE*. 2020; 15(7). doi: 10.1371/journal.pone.0236860.
- 964 **Li MY**, Muldowney JS. Global stability for the SEIR model in epidemiology. *Mathematical Biosciences*. 1995;
965 125(2):155–164. doi: 10.1016/0025-5564(95)92756-5.
- 966 **Lombardo G**, Pellegrino M, Tomaiuolo M, Cagnoni S, Mordonini M, Giacobini M, Poggi A. Fine-Grained Agent-
967 Based Modeling to Predict Covid-19 Spreading and Effect of Policies in Large-Scale Scenarios. *IEEE Journal*
968 *of Biomedical and Health Informatics*. 2022; 26(5):2052–2062. [https://ieeexplore.ieee.org/abstract/document/
969 9737382](https://ieeexplore.ieee.org/abstract/document/9737382), doi: 10.1109/JBHI.2022.3160243.
- 970 **Lorig F**, Johansson E, Davidsson P. Agent-based social simulation of the Covid-19 pandemic: A systematic
971 review. *Journal of Artificial Societies and Social Simulation*. 2021; 24(3):5. doi: 10.18564/jasss.4601.
- 972 **Macal CM**. Everything you need to know about agent-based modelling and simulation. *Journal of Simulation*.
973 2016; 10(2):144–156. doi: 10.1057/jos.2016.7.
- 974 **Marshall BD**. Agent-based modeling. In: El-Sayed AM, Galea S, editors. *Systems science and population health*
975 New York: Oxford University Press; 2017.p. 87–98. doi: 10.1093/acprof:oso/9780190492397.003.0008.
- 976 **Merino MG**, Marinescu MC, Cascajo A, Carretero J, Singh DE. Evaluating the Spread of Omicron COVID-19
977 Variant in Spain. *Future Generation Computer Systems*. 2023; 149:547–561. [https://www.sciencedirect.com/
978 science/article/pii/S0167739X23002753](https://www.sciencedirect.com/science/article/pii/S0167739X23002753), doi: 10.1016/j.future.2023.07.025.
- 979 **Millington JDA**, O’Sullivan D, Perry GLW. Model histories: Narrative explanation in generative simulation mod-
980 elling. *Geoforum*. 2012; 43(6):1025–1034. doi: 10.1016/j.geoforum.2012.06.017.
- 981 **Ministerstwo Zdrowia**, Pierwszy przypadek koronawirusa w Polsce [The first coronavirus case in Poland]; 2020.
982 Available from <https://www.gov.pl/web/zdrowie/pierwszy-przypadek-koronawirusa-w-polsce>.
- 983 **MONID - MOdeling Network for severe Infectious Diseases**, OptimAgent-Eng – Modellierungsnetz Für
984 Schwere Infektionskrankheiten; 2023. Available from [https://webszh.uk-halle.de/monid/?page_id=2028&
985 lang=en](https://webszh.uk-halle.de/monid/?page_id=2028&lang=en).

- 986 **Msemburi W**, Karlinsky A, Knutson V, Aleshin-Guendel S, Chatterji S, Wakefield J. The WHO Estimates of Excess
987 Mortality Associated with the COVID-19 Pandemic. *Nature*. 2023; 613(7942):130–137. <https://www.nature.com/articles/s41586-022-05522-2>, doi: 10.1038/s41586-022-05522-2.
- 989 **Müller SA**, Balmer M, Charlton W, Ewert R, Neumann A, Rakow C, Schlenther T, Nagel K. Predicting the Effects
990 of COVID-19 Related Interventions in Urban Settings by Combining Activity-Based Modelling, Agent-Based
991 Simulation, and Mobile Phone Data. *PLOS ONE*. 2021; 16(10):e0259037. <https://journals.plos.org/plosone/article?id=10.1371/journal.pone.0259037>, doi: 10.1371/journal.pone.0259037.
- 993 **National Institute of Public Health**, Ogólnopolskie Badanie Seroepidemiologiczne COVID-19 OBSER-CO Pod-
994 sumowanie wyników II tury badania [Nationwide Seroepidemiological Study COVID -19 OBSER-CO. Summary
995 of the results of the 2nd round of the study]. Warszawa: National Institute of Public Health; 2021. Report at
996 <https://www.pzh.gov.pl/download/28465/>.
- 997 **National Institute of Public Health**, Ogólnopolskie Badanie Seroepidemiologiczne COVID-19: OBSER-CO.
998 Raport końcowy z badania [Nationwide Seroepidemiological Study COVID-19: OBSER-CO. Final report.].
999 Warszawa: National Institute of Public Health; 2023. Report at <https://www.pzh.gov.pl/wp-content/uploads/2023/02/OBSERCO-Raport-koncowy-z-badania.pdf>.
- 1001 **Niedzialewski K**, Nowosielski JM, Bartczuk RP, Dreger F, Górski Ł, Gruzziel-Słomka M, Kaczorek A, Kisielewski J,
1002 Krupa B, Moszyński A, Radwan M, Semenjuk M, Zieliński J, Rakowski F, The Overview, Design Concepts and
1003 Details Protocol of ICM Epidemiological Model (PDYN 1.5). Rochester, NY: Social Science Research Network;
1004 2022. doi: 10.2139/ssrn.4039054. Preprint at <https://doi.org/10.2139/ssrn.4039054>.
- 1005 **Novakovic A**, Marshall AH. The CP-ABM Approach for Modelling COVID-19 Infection Dynamics and Quan-
1006 tifying the Effects of Non-pharmaceutical Interventions. *Pattern Recognition*. 2022; 130:108790. <https://www.sciencedirect.com/science/article/pii/S0031320322002710>, doi: 10.1016/j.patcog.2022.108790.
- 1008 **Pałka P**, Olszewski R, Kęsik-Brodacka M, Wendland A, Nowak K, Szczepankowska-Bednarek U, Liebers DT. Us-
1009 ing multiagent modeling to forecast the spatiotemporal development of the COVID-19 pandemic in Poland.
1010 *Scientific Reports*. 2022; 12(1):11314. doi: 10.1038/s41598-022-15605-9.
- 1011 **Petrilli CM**, Jones SA, Yang J, Rajagopalan H, O'Donnell L, Chernyak Y, Tobin KA, Cerfolio RJ, Francois F, Horwitz LI.
1012 Factors associated with hospital admission and critical illness among 5279 people with coronavirus disease
1013 2019 in New York City: Prospective cohort study. *BMJ*. 2020; doi: 10.1136/bmj.m1966.
- 1014 **Pinkas J**, Jankowski M, Szumowski Ł, Lusawa A, Zgliczyński WS, Raciborski F, Wierzba W, Gujski M. Public health
1015 interventions to mitigate early spread of SARS-CoV-2 in Poland. *Medical Science Monitor*. 2020; 26. doi:
1016 10.12659/MSM.924730.
- 1017 **Postnikov EB**. Estimation of COVID-19 dynamics “on a back-of-envelope”: Does the simplest SIR model
1018 provide quantitative parameters and predictions? *Chaos, Solitons & Fractals*. 2020; 135:109841. doi:
1019 10.1016/j.chaos.2020.109841.
- 1020 **Priesemann V**, Meyer-Hermann M, Pigeot I, Schöbel A. Der Beitrag von epidemiologischen Mod-
1021 ellen zur Beschreibung des Ausbruchsgeschehens der COVID-19-Pandemie. *Bundesgesundheitsblatt -*
1022 *Gesundheitsforschung - Gesundheitsschutz*. 2021; 64(9):1058–1066. <https://link.springer.com/10.1007/s00103-021-03390-1>, doi: 10.1007/s00103-021-03390-1.
- 1024 **Pueyo T**, Coronavirus: The Hammer and the Dance; 2020. Available from <https://tomaspueyo.medium.com/coronavirus-the-hammer-and-the-dance-be9337092b56>.
- 1026 **Railsback SF**, Grimm V. Agent-Based and Individual-Based Modeling: A Practical Introduction. 2 ed. Princeton
1027 University Press; 2019.
- 1028 **Rakowski F**, Gruzziel M, Bieniasz-Krzywiec Ł, Radomski JP. Influenza epidemic spread simulation for Poland
1029 — a large scale, individual based model study. *Physica A: Statistical Mechanics and its Applications*. 2010;
1030 389(16):3149–3165. doi: 10.1016/j.physa.2010.04.029.
- 1031 **Rakowski F**, Gruzziel M, Krych M, Radomski JP. Large scale daily contacts and mobility model - an individual-
1032 based countrywide simulation study for Poland. *Journal of Artificial Societies and Social Simulation*. 2010;
1033 13(1):13. doi: 10.18564/jasss.152.
- 1034 **Regulski P**, Wendykier P, Kantiem K, Murdzek W. Advanced methods of visual analysis and visualization of
1035 various aspects of the COVID-19 outbreak in Poland. *Procedia Computer Science*. 2021; 192:4194–4199. doi:
1036 10.1016/j.procs.2021.09.195.

- 1037 **Rewerska-Juško M**, Rejda K. Social Stigma of Patients Suffering from COVID-19: Challenges for Health Care
1038 System. *Healthcare*. 2022; 10(2):292. doi: 10.3390/healthcare10020292.
- 1039 **Richiardi M**. The Missing Link: AB Models and Dynamic Microsimulation. In: Leitner S, Wall F, editors. *Artificial*
1040 *Economics and Self Organization* Springer; 2014.p. 3–15. http://link.springer.com/10.1007/978-3-319-00912-4_1,
1041 doi: 10.1007/978-3-319-00912-4_1.
- 1042 **Rippinger C**, Bicher M, Urach C, Brunmeir D, Weibrecht N, Zauner G, Sroczynski G, Jahn B, Mühlberger N, Siebert
1043 U, Popper N. Evaluation of undetected cases during the COVID-19 epidemic in Austria. *BMC Infectious*
1044 *Diseases*. 2021; 21(1):70. doi: 10.1186/s12879-020-05737-6.
- 1045 **Ritchie H**, Mathieu E, Rodés-Guirao L, Appel C, Giattino C, Ortiz-Ospina E, Hasell J, Macdonald B, Beltekian D,
1046 Roser M, Coronavirus pandemic (COVID-19); 2020. Data at <https://ourworldindata.org/coronavirus>.
- 1047 **Sayampanathan AA**, Heng CS, Pin PH, Pang J, Leong TY, Lee VJ. Infectivity of asymptomatic versus symptomatic
1048 COVID-19. *The Lancet*. 2021; 397(10269):93–94. doi: 10.1016/S0140-6736(20)32651-9.
- 1049 **Scobie HM**, Johnson AG, Suthar AB, Severson R, Alden NB, Balter S, Bertolino D, Blythe D, Brady S, Cadwell B,
1050 Cheng I, Davidson S, Delgadillo J, Devinney K, Duchin J, Duwell M, Fisher R, Fleischauer A, Grant A, Griffin J,
1051 et al. Monitoring Incidence of COVID-19 Cases, Hospitalizations, and Deaths, by Vaccination Status—13 U.S.
1052 Jurisdictions, April 4–July 17, 2021. *MMWR Morbidity and Mortality Weekly Report*. 2021; 70(37):1284–1290.
1053 doi: 10.15585/mmwr.mm7037e1.
- 1054 **Shahriari B**, Swersky K, Wang Z, Adams RP, de Freitas N. Taking the Human Out of the Loop: A Review of
1055 Bayesian Optimization. *Proceedings of the IEEE*. 2016; 104(1):148–175. doi: 10.1109/JPROC.2015.2494218.
- 1056 **Sherratt K**, Gruson H, Grah R, Johnson H, Niehus R, Prasse B, Sandmann F, Deuschel J, Wolfram D, Abbott S,
1057 Ullrich A, Gibson G, Ray EL, Reich NG, Sheldon D, Wang Y, Wattanachit N, Wang L, Trnka J, Obozinski G, et al.
1058 Predictive performance of multi-model ensemble forecasts of COVID-19 across European nations. *eLife*.
1059 2023; 12. doi: 10.7554/eLife.81916.
- 1060 **Silverman E**, Gostoli U, Picascia S, Almagor J, McCann M, Shaw R, Angione C. Situating agent-based modelling
1061 in population health research. *Emerging Themes in Epidemiology*. 2021; 18(1):10. doi: 10.1186/s12982-021-
1062 00102-7.
- 1063 **Singh DE**, Luceron CO, Sanchez AL, Merino MG, Gonzalez CD, Delgado-Sanz C, Gomez-Barroso D, Carretero
1064 J, Marinescu MC. Evaluation of vaccination Strategies for the Metropolitan Area of Madrid via Agent-
1065 Based Simulation. *BMJ Open*. 2022; 12(12):e065937. <https://bmjopen.bmj.com/content/12/12/e065937>, doi:
1066 10.1136/bmjopen-2022-065937.
- 1067 **Statistics Poland**, Statistical Yearbook of the Republic of Poland. Warszawa: Statistics Poland; 2019.
1068 Report at [https://stat.gov.pl/download/gfx/portalinformacyjny/pl/defaultaktualnosci/5515/2/19/1/rocznik_](https://stat.gov.pl/download/gfx/portalinformacyjny/pl/defaultaktualnosci/5515/2/19/1/rocznik_statystyczny_rzeczypospolitej_polskiej_2019.pdf)
1069 [statystyczny_rzeczypospolitej_polskiej_2019.pdf](https://stat.gov.pl/download/gfx/portalinformacyjny/pl/defaultaktualnosci/5515/2/19/1/rocznik_statystyczny_rzeczypospolitej_polskiej_2019.pdf).
- 1070 **Tran BX**, Vu GT, Le HT, Pham HQ, Phan HT, Latkin CA, Ho RC. Understanding health seeking behaviors to
1071 inform COVID-19 surveillance and detection in resource-scarce settings. *Journal of Global Health*. 2020;
1072 10(2):0203106. doi: 10.7189/jogh.10.0203106.
- 1073 **Twohig KA**, Nyberg T, Zaidi A, Thelwall S, Sinnathamby MA, Aliabadi S, Seaman SR, Harris RJ, Hope R, Lopez-
1074 Bernal J, Gallagher E, Charlett A, De Angelis D, Presanis AM, Dabrera G, Koshy C, Ash A, Wise E, Moore N, Mori
1075 M, et al. Hospital admission and emergency care attendance risk for SARS-CoV-2 delta (B.1.617.2) compared
1076 with alpha (B.1.1.7) variants of concern: A cohort study. *The Lancet Infectious Diseases*. 2022; 22(1):35–42.
1077 doi: 10.1016/S1473-3099(21)00475-8.
- 1078 **Vincenot CE**. How New Concepts Become Universal Scientific Approaches: Insights from Citation Net-
1079 work Analysis of Agent-Based Complex Systems Science. *Proceedings of the Royal Society B: Biologi-*
1080 *cal Sciences*. 2018; 285(1874):20172360. <https://royalsocietypublishing.org/doi/10.1098/rspb.2017.2360>, doi:
1081 10.1098/rspb.2017.2360.
- 1082 **Walkowiak MP**, Walkowiak D. Underestimation in Reporting Excess COVID-19 Death Data in Poland during
1083 the First Three Pandemic Waves. *International Journal of Environmental Research and Public Health*. 2022;
1084 19(6):3692. doi: 10.3390/ijerph19063692.

- 1085 **Wang H**, Paulson KR, Pease SA, Watson S, Comfort H, Zheng P, Aravkin AY, Bisignano C, Barber RM, Alam T,
1086 Fuller JE, May EA, Jones DP, Frisch ME, Abbafati C, Adolph C, Allorant A, Amlag JO, Bang-Jensen B, Bertolacci
1087 GJ, et al. Estimating Excess Mortality Due to the COVID-19 Pandemic: A Systematic Analysis of COVID-19-
1088 related Mortality, 2020–21. *The Lancet*. 2022; 399(10334):1513–1536. [https://www.thelancet.com/article/
1089 S0140-6736\(21\)02796-3/fulltext](https://www.thelancet.com/article/S0140-6736(21)02796-3/fulltext), doi: 10.1016/S0140-6736(21)02796-3.
- 1090 **Wolfram D**, Abbott S, an der Heiden M, Funk S, Günther F, Hailer D, Heyder S, Hotz T, van de Kasstelee J, Küchen-
1091 hoff H, Müller-Hansen S, Syliqi D, Ullrich A, Weigert M, Schienle M, Bracher J. Collaborative Nowcasting of
1092 COVID-19 Hospitalization Incidences in Germany. *PLOS Computational Biology*. 2023; 19(8):e1011394. [https:
1093 //journals.plos.org/ploscompbiol/article?id=10.1371/journal.pcbi.1011394](https://journals.plos.org/ploscompbiol/article?id=10.1371/journal.pcbi.1011394), doi: 10.1371/journal.pcbi.1011394.
- 1094 **Wong LP**, Wu Q, Hao Y, Chen X, Chen Z, Alias H, Shen M, Hu J, Duan S, Zhang J, Han L. The role of institutional
1095 trust in preventive practices and treatment-seeking intention during the coronavirus disease 2019 outbreak
1096 among residents in Hubei, China. *International Health*. 2022; 14(2):161–169. doi: 10.1093/inthealth/ihab023.
- 1097 **Wolf SH**, Chapman DA, Sabo RT, Weinberger DM, Hill L. Excess Deaths From COVID-19 and Other
1098 Causes, March–April 2020. *JAMA*. 2020; 324(5):510–513. <https://doi.org/10.1001/jama.2020.11787>, doi:
1099 10.1001/jama.2020.11787.
- 1100 **Wu JT**, Leung K, Lam TTY, Ni MY, Wong CKH, Peiris JSM, Leung GM. Nowcasting epidemics of novel pathogens:
1101 Lessons from COVID-19. *Nature Medicine*. 2021; 27(3):388–395. doi: 10.1038/s41591-021-01278-w.
- 1102 **Zhao H**, Lu X, Deng Y, Tang Y, Lu J. COVID-19: asymptomatic carrier transmission is an underestimated problem.
1103 *Epidemiology and Infection*. 2020; 148. doi: 10.1017/S0950268820001235.
- 1104 **Zheng W**, Kämpfen F, Huang Z. Health-seeking and diagnosis delay and its associated factors: A case study on
1105 COVID-19 infections in Shaanxi Province, China. *Scientific Reports*. 2021; 11(1):17331. doi: 10.1038/s41598-
1106 021-96888-2.

1107 **Appendix 1**

1108 **Mitigation measures during the COVID-19 epidemic in Poland**

1109 **Appendix 1—table 1.** Timeline of critical mitigation measures implemented in Poland during the
 1110 COVID-19 pandemic from March 2020 to December 2022

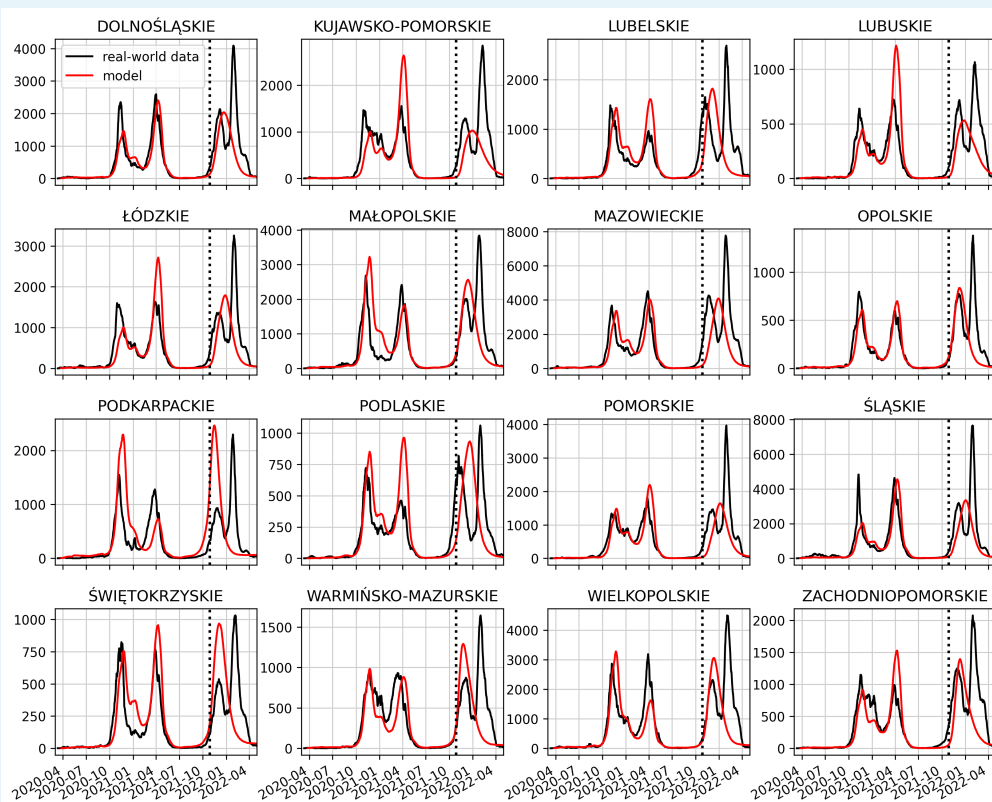
Mitigation measure	Date first introduced
Quarantine for contacts	March 4, 2020
Case detection (testing)	March 4, 2020
Work-from-home order	March 8, 2020
Ban on mass gatherings	March 10, 2020
Online schooling	March 12, 2020
Online studying at universities	March 12, 2020
Ban on entertainment events	March 14, 2020
Closure of sports gyms	March 14, 2020
Closure of hotel accommodations	March 14, 2020
1112 Limits on the number of people in public spaces	March 15, 2020
Closure of public spaces	March 15, 2020
Stay-at-home order	March 24, 2020
Mandatory mask wearing in closed spaces	May 30, 2020
Restrictions on private gatherings	April 2, 2020
Mandatory mask wearing in open spaces	April 14, 2020
Limits in places of worship	April 19, 2020
Limits on sports gyms	June 5, 2020
Limits on hotel accommodations	October 24, 2020
Vaccination programme	December 27, 2020
Availability of booster dose vaccination	November 2, 2021

Appendix 1—table 2. Ranks description for unified restrictions calendar in Poland

Rank	Type of restriction				
	Public space	Workplaces (services)	Universities	Schools	Kindergartens
0	No restrictions.	No restrictions.	No restrictions.	No restrictions.	No restrictions.
1	Social distancing, personal protective equipment, sanitation stations in buildings are required. Gatherings and some mass events are permitted with limits.	Social distancing, personal protective equipment, sanitation stations in buildings are required. Indoor gyms are available with limits.	Social distancing, personal protective equipment, sanitation stations in buildings are required.	Stationary education with social distancing, personal protective equipment, sanitation stations in buildings are required.	Social distancing, personal protective equipment, sanitation stations in buildings are required.
2	Public transport available with additional safety rules. Medium gatherings (approximately 100 persons) are permitted with limits (e.g., weddings).	Some capacity limits in shopping malls. Hospitality and wellness industry are available with limits. Restaurants are available with limits.	Digital learning/remote lectures are default/highly recommended, but face-to-face courses are available.	Different grades are visiting school alternately or hybrid education.	Partial availability depending on local regulations, additional safety norms, and maximum kids capacity limits.
3	Some public spaces like museums, libraries are available. Public transport limited to approximately 50% available seats. Small gatherings are permitted with limits and additional safety norms (<50 persons).	Capacity limits in shopping malls. Hospitality industry, therapeutic rehabilitation is available with strict limits. Indoor wellness industry, swimming pools are closed or strictly limited. Restaurants are strictly limited or can serve only takeaway food.	Digital learning/remote lectures are default, and face-to-face courses are strongly discouraged.	Face-to-face teaching is available only for certain grades (e.g., I-III), specialized courses (e.g., vocational classes), or final exam candidates (e.g., maturity exam).	Kindergartens are available only for kids of medical service parents.
4	Mobility is restricted to commuting or basic necessities of life. Public gathering is forbidden (limit <5 persons). Public transport limited to 25-50% available seats. Underage are not permitted to walk alone.	Shopping malls are closed or strictly limited. Hospitality and wellness industry are fully suspended. The number of people in shops and service points are strictly limited to the number of till points and surface of the point. Restaurants can serve only takeaway food.	Suspension of face-to-face teaching and transition to digital learning.	Suspension of face-to-face teaching and full transition to digital learning.	Kindergartens are suspended.

1117

Forecast on regional level



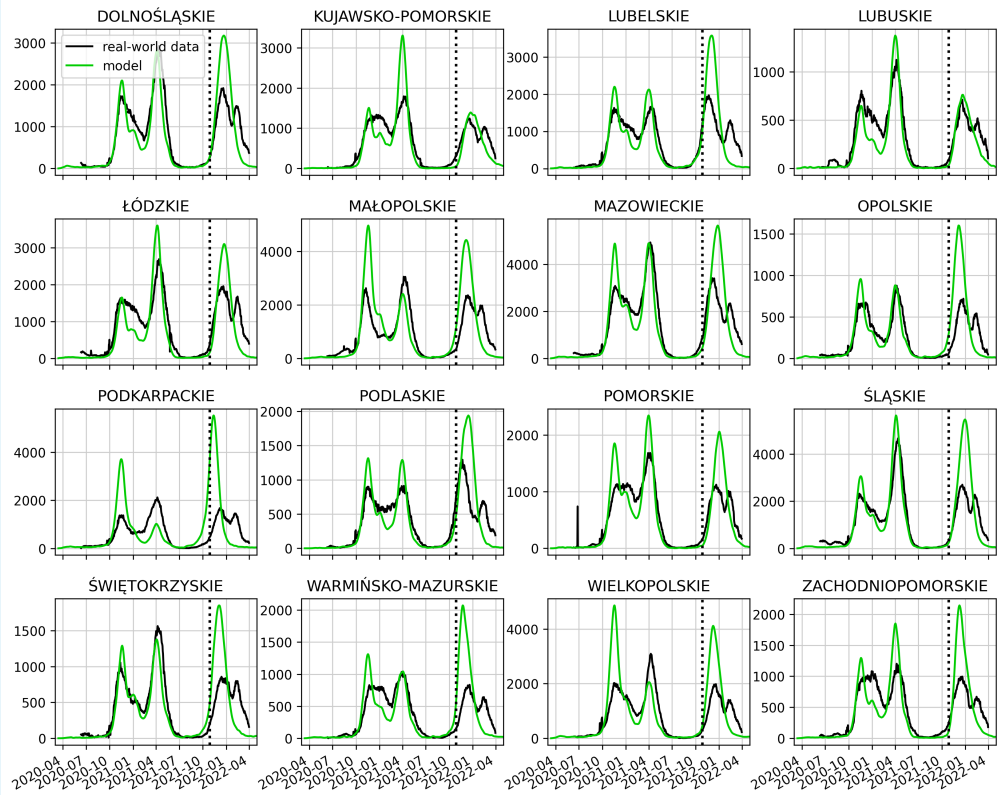
1118

1119

1120

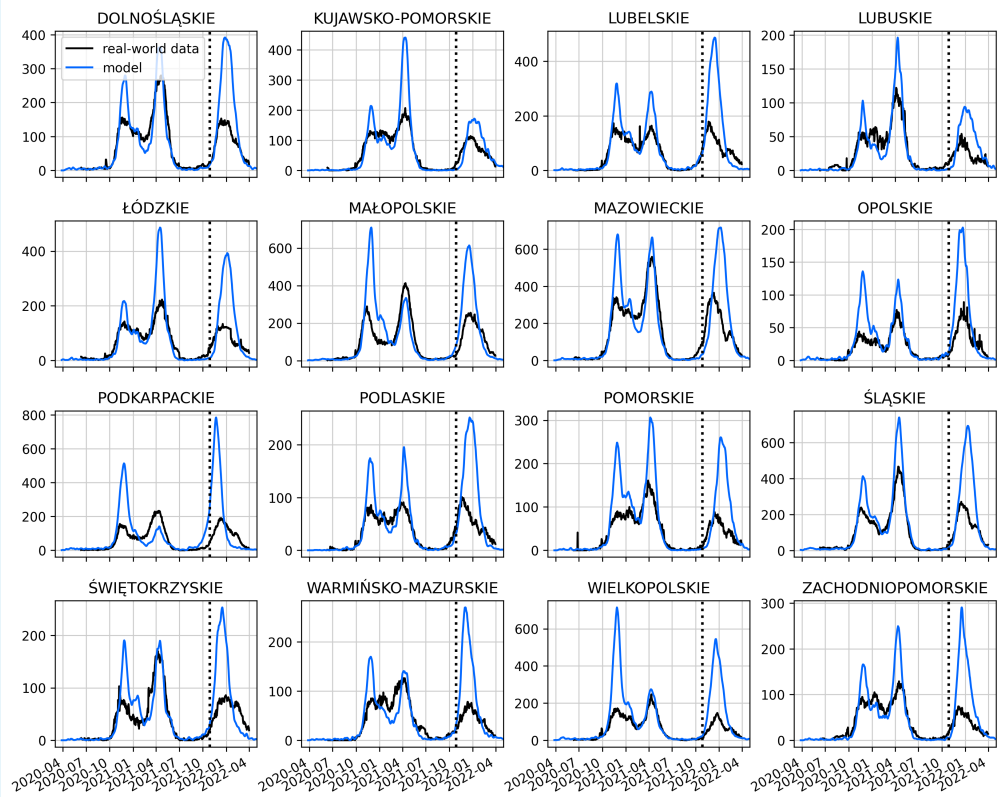
1122

Appendix 2—figure 1. The full course of the COVID-19 detected cases in voivodships: comparison between the dynamics generated from the model (red lines) and the epidemiological data (black lines).



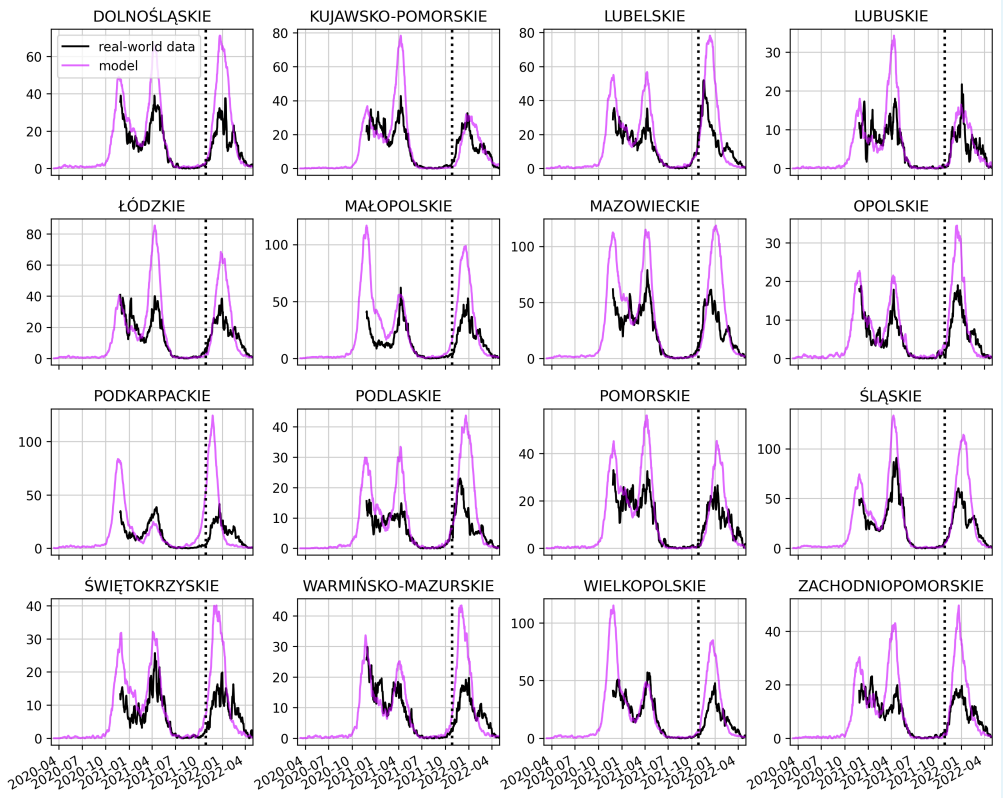
1123
1124
1125
1126

Appendix 2—figure 2. The full course of the COVID-19-related hospitalizations in voivodships: comparison between the dynamics generated from the model (green lines) and the epidemiological data (black lines).



1128
1129
1130
1132

Appendix 2—figure 3. The full course of the COVID-19-related ICU occupation in voivodships: comparison between the dynamics generated from the model (blue lines) and the epidemiological data (black lines).



1133
1134
1135
1136

Appendix 2—figure 4. The full course of the COVID-19-related deaths in voivodships: comparison between the dynamics generated from the model (purple lines) and the epidemiological data (black lines).

1138
1139
1140

Appendix 2—table 1. The comparison between pDyn simulation results and epidemiological data (see text) for disease-related states regarding the peak value, peak date, and width in terms of the Full-Width Half-Maximum (FWHM) of the Delta wave in Dolnośląskie voivodship.

Output	Comparison	Peak value	Peak timing	Width (FWHM)
New confirmed cases	Simulation	2092	2021-12-10	62
	Real-world	2076	2021-12-03	40
	Difference	16	7	22
	Relative difference	0.77%		55.0%
Hospitalized	Simulation	3270	2021-12-21	59
	Real-world	1836	2021-12-15	55
	Difference	1434	6	4
	Relative difference	78.1%		7.27%
ICU patients	Simulation	410	2021-12-30	58
	Real-world	160	2021-12-20	60
	Difference	250	10	-2
	Relative difference	156.25%		-3.33%
Reported deaths	Simulation	70	2021-12-27	60
	Real-world	29	2021-12-24	55
	Difference	41	3	5
	Relative difference	141.38%		9.09%
Excess deaths	Simulation	70	2021-12-27	60
	Real-world	66	2021-12-16	60
	Difference	4	11	0
	Relative difference	6.06%		0.0%

1144

1142
1143

1145
1146
1148

Appendix 2—table 2. The comparison between pDyn simulation results and epidemiological data (see text) for disease-related states regarding the peak value, peak date, and width in terms of the Full-Width Half-Maximum (FWHM) of the Delta wave in Dolnośląskie voivodship.

1151

1149
1150

Output	Comparison	Peak value	Peak timing	Width (FWHM)
New confirmed cases	Simulation	2092	2021-12-10	62
	Real-world	2076	2021-12-03	40
	Difference	16	7	22
	Relative difference	0.77%		55.0%
Hospitalized	Simulation	3270	2021-12-21	59
	Real-world	1836	2021-12-15	55
	Difference	1434	6	4
	Relative difference	78.1%		7.27%
ICU patients	Simulation	410	2021-12-30	58
	Real-world	160	2021-12-20	60
	Difference	250	10	-2
	Relative difference	156.25%		-3.33%
Reported deaths	Simulation	70	2021-12-27	60
	Real-world	29	2021-12-24	55
	Difference	41	3	5
	Relative difference	141.38%		9.09%
Excess deaths	Simulation	70	2021-12-27	60
	Real-world	66	2021-12-16	60
	Difference	4	11	0
	Relative difference	6.06%		0.0%

1152
1153
1155

Appendix 2—table 3. The comparison between pDyn simulation results and epidemiological data (see text) for disease-related states regarding the peak value, peak date, and width in terms of the Full-Width Half-Maximum (FWHM) of the Delta wave in Kujawsko-Pomorskie voivodship.

Output	Comparison	Peak value	Peak timing	Width (FWHM)
New confirmed cases	Simulation	1048	2021-12-11	79
	Real-world	1318	2021-12-01	41
	Difference	-270	10	38
	Relative difference	-20.49%		92.68%
Hospitalized	Simulation	1426	2021-12-20	74
	Real-world	1179	2021-12-15	66
	Difference	247	5	8
	Relative difference	20.95%		12.12%
ICU patients	Simulation	177	2021-12-28	73
	Real-world	107	2021-12-18	64
	Difference	70	10	9
	Relative difference	65.42%		14.06%
Reported deaths	Simulation	31	2021-12-28	74
	Real-world	27	2021-12-19	58
	Difference	4	9	16
	Relative difference	14.81%		27.59%
Excess deaths	Simulation	31	2021-12-28	74
	Real-world	45	2021-12-13	60
	Difference	-14	15	14
	Relative difference	-31.11%		23.33%

1158

1156
1157

1159
1160
1162

Appendix 2—table 4. The comparison between pDyn simulation results and epidemiological data (see text) for disease-related states regarding the peak value, peak date, and width in terms of the Full-Width Half-Maximum (FWHM) of the Delta wave in Lubelskie voivodship.

Output	Comparison	Peak value	Peak timing	Width (FWHM)
New confirmed cases	Simulation	1824	2021-11-22	55
	Real-world	1550	2021-11-10	49
	Difference	274	12	6
	Relative difference	17.68%		12.24%
Hospitalized	Simulation	3663	2021-11-30	53
	Real-world	1938	2021-11-22	59
	Difference	1725	8	-6
	Relative difference	89.01%		-10.17%
ICU patients	Simulation	486	2021-12-11	52
	Real-world	157	2021-11-24	56
	Difference	329	17	-4
	Relative difference	209.55%		-7.14%
Reported deaths	Simulation	79	2021-12-10	55
	Real-world	45	2021-11-26	52
	Difference	34	14	3
	Relative difference	75.56%		5.77%
Excess deaths	Simulation	79	2021-12-10	55
	Real-world	68	2021-11-18	61
	Difference	11	22	-6
	Relative difference	16.18%		-9.84%

1165

1163
1164

1166
1167
1169

Appendix 2—table 5. The comparison between pDyn simulation results and epidemiological data (see text) for disease-related states regarding the peak value, peak date, and width in terms of the Full-Width Half-Maximum (FWHM) of the Delta wave in Lubuskie voivodship.

Output	Comparison	Peak value	Peak timing	Width (FWHM)
New confirmed cases	Simulation	535	2021-12-07	77
	Real-world	683	2021-12-04	37
	Difference	-148	3	40
	Relative difference	-21.67%		108.11%
Hospitalized	Simulation	752	2021-12-16	71
	Real-world	616	2021-12-16	56
	Difference	136	0	15
	Relative difference	22.08%		26.79%
ICU patients	Simulation	94	2021-12-27	71
	Real-world	42	2021-12-19	66
	Difference	52	8	5
	Relative difference	123.81%		7.58%
Reported deaths	Simulation	16	2021-12-22	73
	Real-world	13	2021-12-27	55
	Difference	3	-5	18
	Relative difference	23.08%		32.73%
Excess deaths	Simulation	16	2021-12-22	73
	Real-world	24	2021-12-13	48
	Difference	-8	9	25
	Relative difference	-33.33%		52.08%

1172

1170
1171

1173
1174
1176

Appendix 2—table 6. The comparison between pDyn simulation results and epidemiological data (see text) for disease-related states regarding the peak value, peak date, and width in terms of the Full-Width Half-Maximum (FWHM) of the Delta wave in Łódzkie voivodship.

Output	Comparison	Peak value	Peak timing	Width (FWHM)
New confirmed cases	Simulation	1804	2021-12-14	58
	Real-world	1413	2021-11-30	49
	Difference	391	14	9
	Relative difference	27.67%		18.37%
Hospitalized	Simulation	3153	2021-12-21	55
	Real-world	1968	2021-12-13	62
	Difference	1185	8	-7
	Relative difference	60.21%		-11.29%
ICU patients	Simulation	402	2022-01-01	55
	Real-world	130	2021-12-18	80
	Difference	272	14	-25
	Relative difference	209.23%		-31.25%
Reported deaths	Simulation	67	2021-12-29	58
	Real-world	30	2021-12-20	66
	Difference	37	9	-8
	Relative difference	123.33%		-12.12%
Excess deaths	Simulation	67	2021-12-29	58
	Real-world	58	2021-12-12	62
	Difference	9	17	-4
	Relative difference	15.52%		-6.45%

1179

1177
1178

1180
1181
1183

Appendix 2—table 7. The comparison between pDyn simulation results and epidemiological data (see text) for disease-related states regarding the peak value, peak date, and width in terms of the Full-Width Half-Maximum (FWHM) of the Delta wave in Małopolskie voivodship.

Output	Comparison	Peak value	Peak timing	Width (FWHM)
New confirmed cases	Simulation	2579	2021-11-30	61
	Real-world	2020	2021-12-03	42
	Difference	559	-3	19
	Relative difference	27.67%		45.24%
Hospitalized	Simulation	4499	2021-12-05	58
	Real-world	2165	2021-12-10	51
	Difference	2334	-5	7
	Relative difference	107.81%		13.73%
ICU patients	Simulation	611	2021-12-15	56
	Real-world	225	2021-12-14	54
	Difference	386	1	2
	Relative difference	171.56%		3.7%
Reported deaths	Simulation	98	2021-12-14	60
	Real-world	42	2021-12-18	54
	Difference	56	-4	6
	Relative difference	133.33%		11.11%
Excess deaths	Simulation	98	2021-12-14	60
	Real-world	74	2021-12-13	63
	Difference	24	1	-3
	Relative difference	32.43%		-4.76%

1186

1184
1185

1187
1188
1190

Appendix 2—table 8. The comparison between pDyn simulation results and epidemiological data (see text) for disease-related states regarding the peak value, peak date, and width in terms of the Full-Width Half-Maximum (FWHM) of the Delta wave in Mazowieckie voivodship.

Output	Comparison	Peak value	Peak timing	Width (FWHM)
New confirmed cases	Simulation	4059	2021-12-17	59
	Real-world	4289	2021-11-24	44
	Difference	-230	23	15
	Relative difference	-5.36%		34.09%
Hospitalized	Simulation	5687	2021-12-25	58
	Real-world	3307	2021-12-06	57
	Difference	2380	19	1
	Relative difference	71.97%		1.75%
ICU patients	Simulation	730	2022-01-04	58
	Real-world	359	2021-12-10	65
	Difference	371	25	-7
	Relative difference	103.34%		-10.77%
Reported deaths	Simulation	120	2022-01-02	60
	Real-world	57	2021-12-12	60
	Difference	63	21	0
	Relative difference	110.53%		0.0%
Excess deaths	Simulation	120	2022-01-02	60
	Real-world	121	2021-12-04	62
	Difference	-1	29	-2
	Relative difference	-0.83%		-3.23%

1193

1191
1192

1194
1195
1196
1200
1198
1199

Appendix 2—table 9. The comparison between pDyn simulation results and epidemiological data (see text) for disease-related states regarding the peak value, peak date, and width in terms of the Full-Width Half-Maximum (FWHM) of the Delta wave in Opolskie voivodship.

Output	Comparison	Peak value	Peak timing	Width (FWHM)
New confirmed cases	Simulation	838	2021-11-28	54
	Real-world	786	2021-12-05	40
	Difference	52	-7	14
	Relative difference	6.62%		35.0%
Hospitalized	Simulation	1595	2021-12-06	51
	Real-world	697	2021-12-18	51
	Difference	898	-12	0
	Relative difference	128.84%		0.0%
ICU patients	Simulation	204	2021-12-16	50
	Real-world	72	2021-12-21	60
	Difference	132	-5	-10
	Relative difference	183.33%		-16.67%
Reported deaths	Simulation	33	2021-12-17	53
	Real-world	17	2021-12-17	52
	Difference	16	0	1
	Relative difference	94.12%		1.92%
Excess deaths	Simulation	33	2021-12-17	53
	Real-world	30	2021-12-13	46
	Difference	3	4	7
	Relative difference	10.0%		15.22%

1201
1202
1203
1204
1205
1206
1207

Appendix 2—table 10. The comparison between pDyn simulation results and epidemiological data (see text) for disease-related states regarding the peak value, peak date, and width in terms of the Full-Width Half-Maximum (FWHM) of the Delta wave in Podkarpackie voivodship.

Output	Comparison	Peak value	Peak timing	Width (FWHM)
New confirmed cases	Simulation	2428	2021-11-03	44
	Real-world	915	2021-11-27	49
	Difference	1513	-24	-5
	Relative difference	165.36%		-10.2%
Hospitalized	Simulation	5479	2021-11-12	43
	Real-world	1584	2021-12-07	59
	Difference	3895	-25	-16
	Relative difference	245.9%		-27.12%
ICU patients	Simulation	751	2021-11-23	42
	Real-world	182	2021-12-12	63
	Difference	569	-19	-21
	Relative difference	312.64%		-33.33%
Reported deaths	Simulation	116	2021-11-23	46
	Real-world	31	2021-12-13	54
	Difference	85	-20	-8
	Relative difference	274.19%		-14.81%
Excess deaths	Simulation	116	2021-11-23	46
	Real-world	54	2021-12-08	68
	Difference	62	-15	-22
	Relative difference	114.81%		-32.35%

1208
1209
1210

Appendix 2—table 11. The comparison between pDyn simulation results and epidemiological data (see text) for disease-related states regarding the peak value, peak date, and width in terms of the Full-Width Half-Maximum (FWHM) of the Delta wave in Podlaskie voivodship.

Output	Comparison	Peak value	Peak timing	Width (FWHM)
New confirmed cases	Simulation	938	2021-12-08	61
	Real-world	754	2021-11-11	48
	Difference	184	27	13
	Relative difference	24.4%		27.08%
Hospitalized	Simulation	1998	2021-12-12	60
	Real-world	1238	2021-11-21	56
	Difference	760	21	4
	Relative difference	61.39%		7.14%
ICU patients	Simulation	261	2021-12-23	59
	Real-world	95	2021-11-26	62
	Difference	166	27	-3
	Relative difference	174.74%		-4.84%
Reported deaths	Simulation	43	2021-12-20	62
	Real-world	21	2021-11-28	47
	Difference	22	22	15
	Relative difference	104.76%		31.91%
Excess deaths	Simulation	43	2021-12-20	62
	Real-world	41	2021-11-22	58
	Difference	2	28	4
	Relative difference	4.88%		6.9%

1214

1212
1213

1215
1216
1218

Appendix 2—table 12. The comparison between pDyn simulation results and epidemiological data (see text) for disease-related states regarding the peak value, peak date, and width in terms of the Full-Width Half-Maximum (FWHM) of the Delta wave in Pomorskie voivodship.

Output	Comparison	Peak value	Peak timing	Width (FWHM)
New confirmed cases	Simulation	1626	2021-12-23	62
	Real-world	1472	2021-12-02	46
	Difference	154	21	16
	Relative difference	10.46%		34.78%
Hospitalized	Simulation	2038	2021-12-31	56
	Real-world	1105	2021-12-17	59
	Difference	933	14	-3
	Relative difference	84.43%		-5.08%
ICU patients	Simulation	260	2022-01-11	54
	Real-world	76	2021-12-16	59
	Difference	184	26	-5
	Relative difference	242.11%		-8.47%
Reported deaths	Simulation	43	2022-01-11	58
	Real-world	19	2021-12-21	55
	Difference	24	21	3
	Relative difference	126.32%		5.45%
Excess deaths	Simulation	43	2022-01-11	58
	Real-world	43	2021-12-18	71
	Difference	0	24	-13
	Relative difference	0.0%		-18.31%

1221

1219
1220

1222
1223
1225

Appendix 2—table 13. The comparison between pDyn simulation results and epidemiological data (see text) for disease-related states regarding the peak value, peak date, and width in terms of the Full-Width Half-Maximum (FWHM) of the Delta wave in Śląskie voivodship.

Output	Comparison	Peak value	Peak timing	Width (FWHM)
New confirmed cases	Simulation	3340	2021-12-21	58
	Real-world	3207	2021-12-04	40
	Difference	133	17	18
	Relative difference	4.15%		45.0%
Hospitalized	Simulation	5536	2021-12-30	55
	Real-world	2624	2021-12-17	54
	Difference	2912	13	1
	Relative difference	110.98%		1.85%
ICU patients	Simulation	689	2022-01-10	55
	Real-world	264	2021-12-20	55
	Difference	425	21	0
	Relative difference	160.98%		0.0%
Reported deaths	Simulation	115	2022-01-07	58
	Real-world	56	2021-12-22	52
	Difference	59	16	6
	Relative difference	105.36%		11.54%
Excess deaths	Simulation	115	2022-01-07	58
	Real-world	116	2021-12-15	54
	Difference	-1	23	4
	Relative difference	-0.86%		7.41%

1228

1226
1227

1229
1230
1232

Appendix 2—table 14. The comparison between pDyn simulation results and epidemiological data (see text) for disease-related states regarding the peak value, peak date, and width in terms of the Full-Width Half-Maximum (FWHM) of the Delta wave in Świętokrzyskie voivodship.

Output	Comparison	Peak value	Peak timing	Width (FWHM)
New confirmed cases	Simulation	974	2021-11-20	57
	Real-world	526	2021-12-01	42
	Difference	448	-11	15
	Relative difference	85.17%		35.71%
Hospitalized	Simulation	1866	2021-12-01	55
	Real-world	812	2021-12-13	61
	Difference	1054	-12	-6
	Relative difference	129.8%		-9.84%
ICU patients	Simulation	249	2021-12-12	55
	Real-world	74	2021-12-16	71
	Difference	175	-4	-16
	Relative difference	236.49%		-22.54%
Reported deaths	Simulation	40	2021-12-08	59
	Real-world	15	2021-12-20	64
	Difference	25	-12	-5
	Relative difference	166.67%		-7.81%
Excess deaths	Simulation	40	2021-12-08	59
	Real-world	25	2021-12-13	81
	Difference	15	-5	-22
	Relative difference	60.0%		-27.16%

1235

1233
1234

1236
1237
1238
1239

Appendix 2—table 15. The comparison between pDyn simulation results and epidemiological data (see text) for disease-related states regarding the peak value, peak date, and width in terms of the Full-Width Half-Maximum (FWHM) of the Delta wave in Warmińsko-Mazurskie voivodship.

Output	Comparison	Peak value	Peak timing	Width (FWHM)
New confirmed cases	Simulation	1278	2021-11-11	54
	Real-world	877	2021-11-28	43
	Difference	401	-17	11
	Relative difference	45.72%		25.58%
Hospitalized	Simulation	2029	2021-11-21	52
	Real-world	803	2021-12-12	57
	Difference	1226	-21	-5
	Relative difference	152.68%		-8.77%
ICU patients	Simulation	263	2021-12-01	51
	Real-world	70	2021-12-16	77
	Difference	193	-15	-26
	Relative difference	275.71%		-33.77%
Reported deaths	Simulation	42	2021-12-02	56
	Real-world	18	2021-12-17	58
	Difference	24	-15	-2
	Relative difference	133.33%		-3.45%
Excess deaths	Simulation	42	2021-12-02	56
	Real-world	31	2021-12-13	61
	Difference	11	-11	-5
	Relative difference	35.48%		-8.2%

1242

1240
1241

1243
1244
1246

Appendix 2—table 16. The comparison between pDyn simulation results and epidemiological data (see text) for disease-related states regarding the peak value, peak date, and width in terms of the Full-Width Half-Maximum (FWHM) of the Delta wave in Wielkopolskie voivodship.

Output	Comparison	Peak value	Peak timing	Width (FWHM)
New confirmed cases	Simulation	3053	2021-11-28	54
	Real-world	2330	2021-12-03	38
	Difference	723	-5	16
	Relative difference	31.03%		42.11%
Hospitalized	Simulation	4075	2021-12-08	53
	Real-world	1900	2021-12-15	54
	Difference	2175	-7	-1
	Relative difference	114.47%		-1.85%
ICU patients	Simulation	522	2021-12-19	52
	Real-world	129	2021-12-22	56
	Difference	393	-3	-4
	Relative difference	304.65%		-7.14%
Reported deaths	Simulation	84	2021-12-19	56
	Real-world	38	2021-12-23	50
	Difference	46	-4	6
	Relative difference	121.05%		12.0%
Excess deaths	Simulation	84	2021-12-19	56
	Real-world	67	2021-12-15	62
	Difference	17	4	-6
	Relative difference	25.37%		-9.68%

1249

1247
1248

1250
1251
1253

Appendix 2—table 17. The comparison between pDyn simulation results and epidemiological data (see text) for disease-related states regarding the peak value, peak date, and width in terms of the Full-Width Half-Maximum (FWHM) of the Delta wave in Zachodniopomorskie voivodship.

Output	Comparison	Peak value	Peak timing	Width (FWHM)
New confirmed cases	Simulation	1328	2021-11-26	57
	Real-world	1255	2021-11-28	43
	Difference	73	-2	14
	Relative difference	5.82%		32.56%
Hospitalized	Simulation	2068	2021-12-05	54
	Real-world	971	2021-12-13	65
	Difference	1097	-8	-11
	Relative difference	112.98%		-16.92%
ICU patients	Simulation	260	2021-12-15	52
	Real-world	67	2021-12-13	66
	Difference	193	2	-14
	Relative difference	288.06%		-21.21%
Reported deaths	Simulation	44	2021-12-16	55
	Real-world	18	2021-12-18	60
	Difference	26	-2	-5
	Relative difference	144.44%		-8.33%
Excess deaths	Simulation	44	2021-12-16	55
	Real-world	36	2021-12-13	71
	Difference	8	3	-16
	Relative difference	22.22%		-22.54%

1256

1254
1255

1258 **Model parameters**1260 **Appendix 3—table 1.** General model parameters.

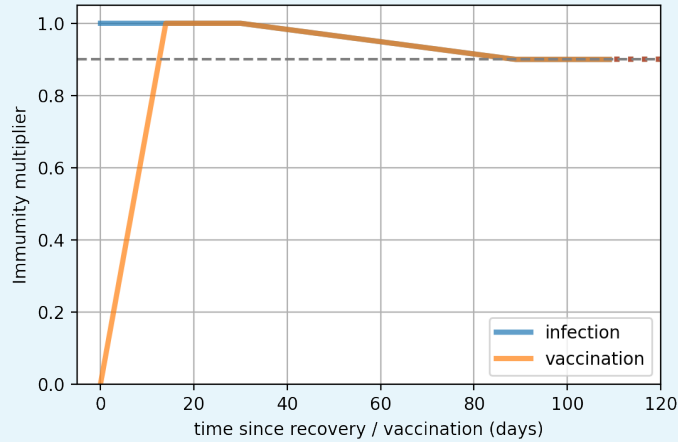
Parameter name	Parameter value
Base virus infectivity (α)	2.047 250
Base fraction of symptomatic agents leaving home (f)	0.403 245
Household contact rate	2.5
School contact rate	1.66
Preschool contact rate	1.66
1261 Workplace contact rate	1.66
University contact rate	1.66
Travel contact rate	1.66
Street contact rate	0.83
Traveller creation rate	0.0005
Asymptomatic agents infectivity multiplier	0.1
Share of asymptomatic agents	0.8

1262 **Appendix 3—table 2.** Cross-immunity matrix. Cross-immunity matrix C of size $(N + M) \times N$ is used to
 1263 represent a cross-immunity phenomenon, where N is the number of variants and M is the number of
 1264 vaccine types. Level of immunity against a new infection (columns), generated by infection recovery or
 1265 a vaccination event (rows), is different for each variant.

Variant	Wild type	Alpha	Delta
Wild type	1	1	0.975
1267 Alpha	1	1	0.975
Delta	0.975	0.975	1
Vaccine	1	1	0.975

1269 **Appendix 3—table 3.** Parameters of new virus variants introduction.

Variant	Introduction date	Number of introduced cases
1270 Wild	06.03.2020	1260
Alpha	25.12.2020	20000
Delta	15.05.2021	5400



1271
1272
1273
1274
1275
1276

Appendix 3—figure 1. Immunity multiplier function. $S(t)$ is an immunity multiplier function, representing immunity decline in time. Immunity is acquired at the moment of recovery or vaccination. Immunity multiplier for vaccines rises from 0 to 1.0 during first 14 days and is equal to 1.0 until day 30. For infections, it is changed to 1.0 immediately after the recovery. In both cases, immunity multiplier decreases linearly from 1.0 on day 30 to 0.9 on day 90 (0.0017 per day).

1279

Appendix 3—table 4. Disease-related states duration.

State name	State duration in days
Latent	4
Asymptomatic	7
Symptomatic	5
Hospitalized, pre-ICU	13
Hospitalized, at ICU	7
Hospitalized, not at ICU	10
Recovered	1

1280

1282

Appendix 3—table 5. State transitions probabilities in different age groups.

State transition	Age range (from inclusive, to exclusive)						
	0–20	20–30	30–40	40–50	50–60	60–70	70+
Latent → Asymptomatic	0.92	0.92	0.84	0.84	0.68	0.63	0.23
Latent → Symptomatic	0.08	0.08	0.16	0.16	0.32	0.37	0.77
Asymptomatic → Recovered	1.0	1.0	1.0	1.0	1.0	1.0	1.0
Symptomatic → Hospitalized, not at ICU	0.02	0.024	0.036	0.07	0.14	0.4	0.5
Symptomatic → Hospitalized, pre-ICU	0.002	0.004	0.006	0.01	0.02	0.1	0.2
Symptomatic → Dead	0.001	0.001	0.002	0.002	0.005	0.02	0.03
Symptomatic → Recovered	0.977	0.971	0.956	0.918	0.835	0.48	0.27
Hospitalized, not at ICU → Dead	0.08	0.08	0.08	0.08	0.08	0.08	0.08
Hospitalized, not at ICU → Recovered	0.92	0.92	0.92	0.92	0.92	0.92	0.92
Hospitalized, pre-ICU → Hospitalized, at ICU	1.0	1.0	1.0	1.0	1.0	1.0	1.0
Hospitalized, at ICU → Dead	0.75	0.75	0.75	0.75	0.75	0.75	0.75
Hospitalized, at ICU → Recovered	0.25	0.25	0.25	0.25	0.25	0.25	0.25

1283

Appendix 3—table 6. Contexts multipliers.

Date	Household multiplier	Kindergarten multiplier	School multiplier	Workplace multiplier	University multiplier	Big university multiplier	Travel multiplier	Street multiplier	Fraction of symptomatic agents leaving home	Travellers creation multiplier	Max. travel duration	Max. travel package	Min. school age	Max. school age
06/03/2020	1	1	1	1	1	1	1	1	1	1	7	40	0	20
12/03/2020	1.01	0.2	0.2	0.8	0	0	1	0.7	1	1	7	40	0	20
14/03/2020	1.02	0.01	0.01	0.5	0	0	1	0.55	0.2	1	7	40	0	20
24/03/2020	1.02	0.01	0.01	0.35	0	0	0.25	0.4	0.1	0.75	7	20	0	20
01/04/2020	1.04	0.01	0.01	0.2	0	0	0.25	0.25	0.03	0.5	7	20	0	20
06/04/2020	1.04	0	0	0.2	0	0	0.25	0.25	0.03	0.5	7	20	0	20
11/04/2020	1.04	0	0	0.2	0	0	0.25	0.15	0.03	0.5	7	20	0	20
16/04/2020	1.04	0	0	0.2	0	0	0.25	0.1	0.03	0.5	7	20	0	20
20/04/2020	1.03	0	0	0.2	0	0	0.27	0.12	0.03	0.5	7	20	0	20
06/05/2020	1.02	0.01	0	0.2	0	0	0.27	0.12	0.03	0.5	7	20	0	20
18/05/2020	1.01	0.01	0.01	0.2	0	0	0.27	0.12	0.03	0.55	7	25	0	20
30/05/2020	1	0.01	0.01	0.2	0	0	0.27	0.12	0.03	0.6	7	25	0	20
26/06/2020	0.95	0.01	0	0.25	0	0	0.27	0.15	0.04	0.6	14	30	0	20
10/07/2020	0.95	0.1	0	0.25	0	0	0.3	0.7	0.05	0.75	14	35	0	20
10/08/2020	0.95	0.1	0	0.25	0	0	0.27	0.4	0.05	0.55	10	35	0	20
03/09/2020	1	0.25	0.25	0.35	0	0	0.27	0.55	0.05	0.55	7	35	0	20
15/09/2020	1	0.35	0.35	0.45	0	0	0.27	0.65	0.05	0.55	7	35	0	20
01/10/2020	1	0.35	0.35	0.54	0.2	0.2	0.27	0.64	0.05	0.55	7	35	0	20
10/10/2020	1	0.3	0.28	0.45	0.2	0.2	0.27	0.45	0.04	0.55	7	30	0	20
17/10/2020	1	0.3	0.26	0.31	0.2	0.2	0.25	0.36	0.03	0.5	7	30	0	20
26/10/2020	1.025	0.3	0.3	0.27	0.1	0.1	0.25	0.3	0.03	0.5	7	25	0	9
31/10/2020	1.03	0.3	0.3	0.2	0.08	0.08	0.25	0.2	0.03	0.5	7	22	0	9
07/11/2020	1.03	0.3	0.02	0.06	0	0	0.25	0.09	0.03	0.5	7	20	0	20
28/11/2020	1.04	0.3	0.02	0.23	0	0	0.25	0.28	0.03	0.5	7	20	0	20
06/12/2020	1.04	0.3	0.02	0.26	0	0	0.25	0.3	0.03	0.5	7	20	0	20
24/12/2020	1.05	0.05	0	0.1	0	0	0.35	0.65	0.03	1	10	25	0	20
28/12/2020	1.04	0.3	0.05	0.15	0	0	0.25	0.19	0.03	0.5	7	20	0	20
13/01/2021	1.04	0.3	0.05	0.2	0	0	0.25	0.2	0.03	0.5	7	20	0	20
18/01/2021	1.03	0.3	0.35	0.22	0	0	0.25	0.23	0.03	0.5	7	20	0	9
01/02/2021	1.03	0.3	0.35	0.28	0.05	0.05	0.25	0.28	0.03	1	7	25	0	9
12/02/2021	1.03	0.3	0.35	0.29	0.05	0.05	0.25	0.29	0.03	2	7	25	0	9
27/02/2021 ¹	1.03	0.3	0.15	0.2	0.01	0.01	0.25	0.2	0.03	1	7	20	0	9
08/03/2021	1.03	0.3	0.35	0.18	0.05	0.05	0.25	0.18	0.03	1	7	25	0	9
09/03/2021 ¹	1.03	0.3	0.15	0.16	0.01	0.01	0.25	0.16	0.03	0.5	7	20	0	9
15/03/2021 ²	1.03	0.3	0.15	0.15	0.01	0.01	0.25	0.15	0.03	0.5	7	20	0	9
20/03/2021	1.04	0.3	0.05	0.12	0.01	0.01	0.25	0.12	0.03	0.5	7	20	0	20
29/03/2021	1.04	0.02	0.02	0.12	0.01	0.01	0.25	0.12	0.03	0.5	7	20	0	20
19/04/2021	1.03	0.3	0.02	0.19	0.01	0.01	0.25	0.2	0.03	0.5	7	20	0	20
25/04/2021	1.03	0.3	0.02	0.2	0.01	0.01	0.25	0.2	0.03	0.5	7	20	0	9
26/04/2021 ³	1.03	0.3	0.15	0.18	0.01	0.01	0.25	0.18	0.03	0.5	7	20	0	9
01/05/2021	1.02	0.3	0	0.17	0.05	0.05	0.25	0.2	0.03	1.5	7	20	0	9
04/05/2021	1.02	0.3	0.1	0.12	0.05	0.05	0.25	0.12	0.03	1	7	20	0	9
08/05/2021	1.01	0.3	0.1	0.1	0.05	0.05	0.27	0.1	0.04	1	7	20	0	9
15/05/2021	1	0.3	0.05	0.05	0.05	0.05	0.27	0.06	0.04	1	7	20	0	20
21/05/2021	1	0.3	0.05	0.04	0.05	0.05	0.27	0.05	0.04	1	7	20	0	20
29/05/2021	1	0.3	0.1	0.04	0.05	0.05	0.27	0.05	0.04	1	7	20	0	20
06/06/2021	1	0.3	0.1	0.05	0.05	0.05	0.27	0.06	0.04	1	7	20	0	20
13/06/2021	1	0.3	0.07	0.08	0.03	0.03	0.27	0.08	0.04	1	7	20	0	20
26/06/2021	0.98	0.3	0	0.2	0	0	0.27	0.25	0.04	2	14	35	0	20
05/08/2021	0.98	0.3	0	0.22	0	0	0.27	0.26	0.04	2	14	35	0	20
15/08/2021	0.98	0.3	0	0.26	0	0	0.27	0.33	0.04	2	14	35	0	20
01/09/2021	1	0.3	0.2	0.28	0.05	0.05	0.25	0.33	0.03	1	7	25	0	20
01/10/2021	1.02	0.3	0.2	0.35	0.8	0.8	0.25	0.4	0.03	1	7	25	0	20
01/11/2021	1.03	0.3	0.2	0.35	0.8	0.8	0.25	0.4	0.03	1	7	25	0	20

1286

¹ in Warmińsko-Mazurskie Voivodeship,

1287

² in Lubuskie, Mazowieckie and Pomorskie Voivodeships,

1288

1289

³ in Kujawsko-Pomorskie, Lubelskie, Lubuskie, Małopolskie, Mazowieckie, Podkarpackie, Podlaskie, Pomorskie, Świętokrzyskie, Warmińsko-Mazurskie and Zachodniopomorskie Voivodeships

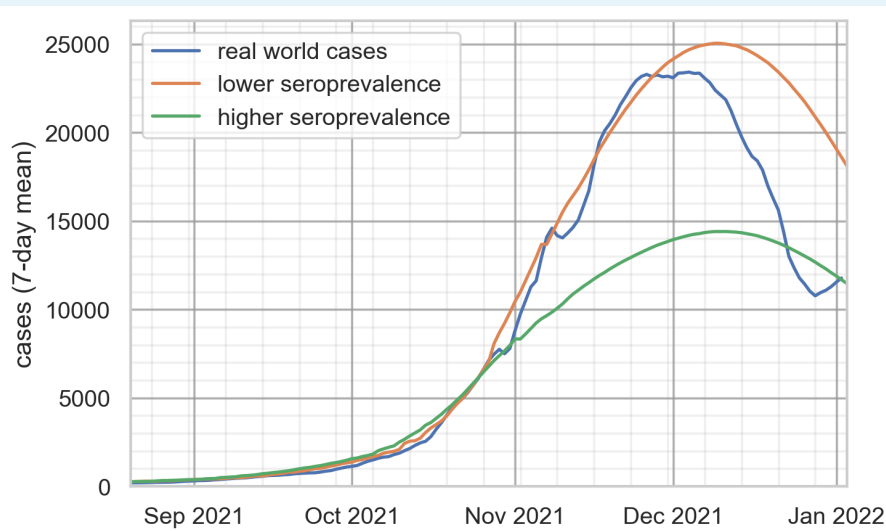
1290

Data sources

Appendix 4—table 1. Input data sources in detail

Data type	Provider	Publicly available	Other
Household structure in Poland	Statistics Poland	No	Under NDA
Age structure in Poland	Statistics Poland	Yes	https://stat.gov.pl
Workplaces in Poland	Statistics Poland	Yes	https://stat.gov.pl
Schools in Poland	Statistics Poland	Yes	https://stat.gov.pl
Universities in Poland	Statistics Poland	Yes	https://stat.gov.pl
COVID-19 classified deaths	Michał Rogalski, Polish Ministry of Health	Yes	<i>Epidemiological Model Team – ICM UW (2023)</i> , https://gov.pl/web/koronawirus/wykaz-zarazen-koronawirusem-sars-cov-2
COVID-19 detected cases	Michał Rogalski, Polish Ministry of Health	Yes	<i>Epidemiological Model Team – ICM UW (2023)</i> , https://gov.pl/web/koronawirus/wykaz-zarazen-koronawirusem-sars-cov-2
COVID-19 hospitalized patients	Michał Rogalski, Polish Ministry of Health	Yes	<i>Epidemiological Model Team – ICM UW (2023)</i> , https://twitter.com/MZ_GOV_PL
COVID-19 severeness of illness (ICU demand)	Michał Rogalski, Polish Ministry of Health	Yes	<i>Epidemiological Model Team – ICM UW (2023)</i> , https://twitter.com/MZ_GOV_PL
COVID-19 time to onset of symptoms	Publications	Yes	?
COVID-19 time of sickness	The National Institute of Public Health	No	Under NDA
COVID-19 time of hospitalization	The National Institute of Public Health	No	Under NDA
Geographically spanned information about COVID-19 detected cases	Polish Ministry of Health	Yes	https://gov.pl/web/koronawirus/wykaz-zarazen-koronawirusem-sars-cov-2
Number of people in quarantine	Polish Ministry of Health	Yes	https://gov.pl/web/koronawirus/wykaz-zarazen-koronawirusem-sars-cov-2
Non-pharmaceutical interventions	Polish Ministry of Health	Yes	https://gov.pl/web/koronawirus
Contact tracing data	The National Institute of Public Health	No	Under NDA
COVID-19 seroprevalence in Poland	The National Institute of Public Health	Yes	https://pzh.gov.pl/projekty-i-programy/obserco/raporty
Initial contacting rates	citation	Yes	-
COVID-19 cross-immunity parameters estimation	<i>Scobie et al. (2021)</i>	Yes	-

1297 **Model calibration**



1298

1299

1300

Appendix 5—figure 1. Optimistic and pessimistic forecast scenarios. Confidence interval produced by running simulation with multiple seeds is too small to be visible.

Determination of peak parameters

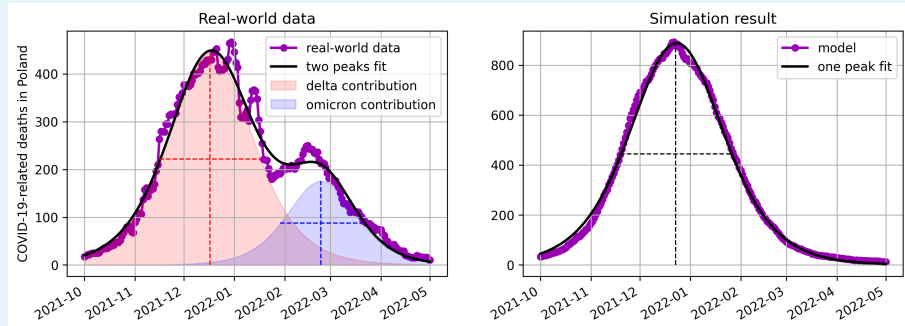
Logistic distribution was used to fit the peak data, in order to determine the peak position, the peak value, and the peak width. Its mathematical formula reads as follows:

$$f(t, t_0, h, w) = \frac{h}{\cosh^2\left(\operatorname{arccosh}(\sqrt{2}) \cdot \frac{t-t_0}{w}\right)}, \quad (1)$$

where t is time, t_0 is peak position, h is peak value, and w is peak width. Because a factor $\operatorname{arccosh}(\sqrt{2}) \approx 0.8814$ is used, the peak width appears as a full-width at half maximum (FWHM) quantity.

The fitting was done using the non-linear least squares method, provided by `curve_fit` tool from the `scipy.optimize` package, yielding the values of t_0 , h , and w , which fit the best for the given data. In case of two-peaks fitting, a sum $f(t, t_1, h_1, w_1) + f(t, t_2, h_2, w_2)$ was used instead, returning best values of 6 parameters.

The examples of two-peaks and one-peak fitting to real-world and simulation result, respectively, for exemplary data of COVID-19-related deaths in Poland, are presented in Figure 1.



Appendix 6—figure 1. Example of fitting the peaks with the logistic distribution, for *delta* (and *omicron*) wave(s) of COVID-19-related deaths in Poland: (a) two-peaks fit to real-world data, (b) one-peak fit to the simulation result. Filled red and blue area in (a) show two contributing peaks. Dashed lines in both panels represent the determined parameters of the peaks: the location of the vertical line for the peak position, its length for the peak value, the length of the horizontal line for the peak width.

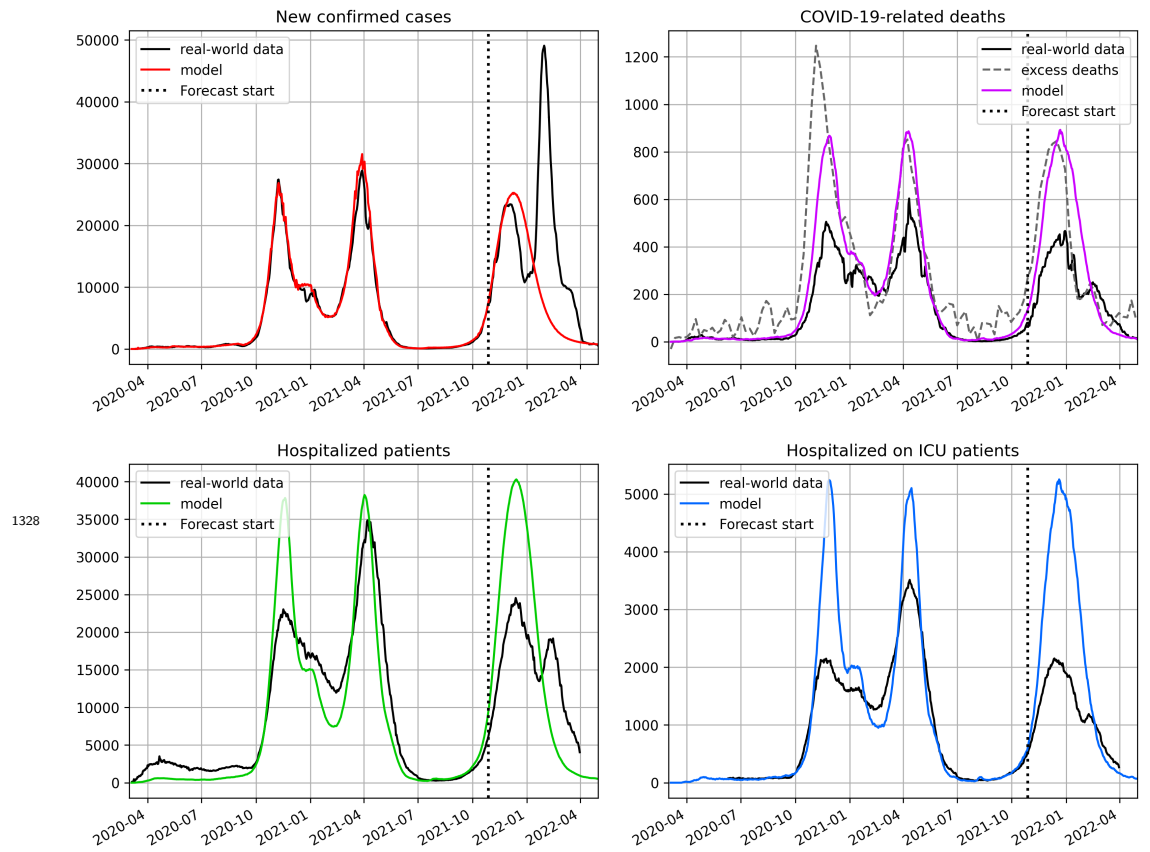


Figure 6—figure supplement 1. Comparison between the pDyn model-generated output (colored lines) and the epidemiological data published by the Polish Ministry of Health (black) and Eurostat (*Eurostat, 2023a*) (dashed grey) for the entire course of the COVID-19 epidemics in Poland. Top left: new confirmed cases. Top right: COVID-19-related deaths. Bottom left: hospitalized patients. Bottom right: ICU patients. The vertical dotted line indicates the simulation date.